

University of Montana

## ScholarWorks at University of Montana

---

Graduate Student Theses, Dissertations, &  
Professional Papers

Graduate School

---

2004

### Comparison of remotely sensed land surface processes in northern hemisphere during the 1988-89 La Nina and the 1997-98 El Nino events

Divya K. Tipparaju  
*The University of Montana*

Follow this and additional works at: <https://scholarworks.umt.edu/etd>

**Let us know how access to this document benefits you.**

---

#### Recommended Citation

Tipparaju, Divya K., "Comparison of remotely sensed land surface processes in northern hemisphere during the 1988-89 La Nina and the 1997-98 El Nino events" (2004). *Graduate Student Theses, Dissertations, & Professional Papers*. 6589.  
<https://scholarworks.umt.edu/etd/6589>

This Thesis is brought to you for free and open access by the Graduate School at ScholarWorks at University of Montana. It has been accepted for inclusion in Graduate Student Theses, Dissertations, & Professional Papers by an authorized administrator of ScholarWorks at University of Montana. For more information, please contact [scholarworks@mso.umt.edu](mailto:scholarworks@mso.umt.edu).



**Maureen and Mike  
MANSFIELD LIBRARY**

The University of  
**Montana**

---

Permission is granted by the author to reproduce this material in its entirety, provided that this material is used for scholarly purposes and is properly cited in published works and reports.

**\*\*Please check "Yes" or "No" and provide signature\*\***

Yes, I grant permission

No, I do not grant permission

Author's Signature: Divya Kulkarni T.

Date: 06/14/2004

Any copying for commercial purposes or financial gain may be undertaken only with the author's explicit consent.

---



**COMPARISON OF REMOTELY SENSED  
LAND SURFACE PROCESSES IN NORTHERN  
HEMISPHERE DURING THE 1988-89 LA  
NIÑA AND THE 1997-98 EL NIÑO EVENTS**

by

Divya. K, Tipparaju

B.E(Civil Engg), Vasavi College of Engineering, Hyderabad, India 2000

Presented in partial fulfillment of the requirements  
for the degree of

Master of Science in Forestry


The University of Montana

August 2004

Approved by:



Chairperson



Dean, Graduate School

8-10-04

Date



UMI Number: EP37390

All rights reserved

INFORMATION TO ALL USERS

The quality of this reproduction is dependent upon the quality of the copy submitted.

In the unlikely event that the author did not send a complete manuscript and there are missing pages, these will be noted. Also, if material had to be removed, a note will indicate the deletion.



UMI EP37390

Published by ProQuest LLC (2013). Copyright in the Dissertation held by the Author.

Microform Edition © ProQuest LLC.

All rights reserved. This work is protected against unauthorized copying under Title 17, United States Code



ProQuest LLC.  
789 East Eisenhower Parkway  
P.O. Box 1346  
Ann Arbor, MI 48106 - 1346

**Comparison of Remotely Sensed Land Surface Processes in Northern Hemisphere during the 1988-89 La Niña and the 1997-98 El Niño events.**

**Director: Dr. Hans Zuuring** 

El Niño and La Niña events are major climatic events disrupting global climatic conditions such as air temperature at different times and scales. The multivariate ENSO Index (MEI) is used to measure the intensity of these events, which showed that 1997-1998 and 1988-1989 were strong El Niño and La Niña events respectively. Terrestrial air temperature controls seasonal freezing and thawing cycles. Freezing and thawing conditions are the transitions between the frozen and non-frozen states of land surface. This transition between the seasonal freezing and thawing affects ground thermal conditions that in turn greatly impact the plant growth.

This study describes the temporal (monthly) variation of the frozen and non-frozen land and examines the linear association among the duration of the frozen land, air temperature and Gross Primary Production (GPP) associated with the 1997-98 El Niño and the 1988-89 La Niña events. The National Snow and Ice Data Center (NSIDC) provided daily freeze/thaw datasets for the Northern Hemisphere. Global monthly average air temperature (°C) data were obtained from the Global Historical Climatology Network (GHCN) Version 2, Legates and Willmott's stations. The daily average GPP data are obtained using the MODIS productivity (MOD17) algorithm that uses the global composite monthly Fraction of Photosynthetically Active Radiation (FPAR).

The temporal extents and the relation among these attributes are described for North America and Northern Eurasia for each event. A non-homogenous distribution of frozen and non-frozen land is identified for both regions and the amount of frozen land is lesser approximately by 0.7 million sq. km for North America and by 0.3 million sq. km for Northern Eurasia during the 1997-98 El Niño event than the 1988-89 La Niña event. During the 1997-98 El Niño, the transition between freezing and thawing shifted a month earlier compared to the 1988-89 La Niña for North America and no such shift occurred for Northern Eurasia.

However, the correlation coefficients between the land surface attributes are found to be almost the same between the two events for both regions. Correlation analysis showed a very strong association between frozen land duration and air temperature and a dispersed relation between frozen land duration and GPP while no clear association was found between air temperature and GPP. The linear relations among the land surface attributes were found to be stronger in North America and weaker in Northern Eurasia (except for frozen land duration Vs air temperature).

The results from graphical displays showed that North America as well as Northern Eurasia had more or less similar variation of air temperature and GPP with in each class of frozen land duration. Nevertheless, Northern Eurasia had lower difference of frozen land area between the two events, had no change in the transition between two events and had weaker correlation among the attributes. Hence, unlike North America, there might be other climatic variations such as North Atlantic Oscillation (NAO) other than MEI affecting the land surface processes of Northern Eurasia.

## ACKNOWLEDGMENTS

I am immensely indebted to **Dr. Ramakrishna Nemani** for supporting me financially throughout this study (MS) and giving me the opportunity to work for him. It was very good experience for me professionally as well as personally.

I am grateful to **Dr. Hans Zuuring** for his time, patience and encouragement in all phases of this project. Without his tremendous help, it would have been much difficult for me to finish it.

I am thankful to **Dr. Brian Steele** for his valuable suggestions and willingness to help.

I would like to thank the members of **NTSG**, especially Steve Running, Cristina Milesi, Faith Ann Heinsch and Hirofumi Hashimoto for the friendliness and all day to day little help that I demanded from them.

I am also greatly indebted to my family for always being with me, guiding and encouraging me. If I had achieved anything or done any good that would be always because of them. With out them, my life would definitely be empty. I owe them throughout my life.

*This project was funded by National Oceanic Atmospheric Administration.*

## TABLE OF CONTENTS

---

ABSTRACT.....	ii
ACKNOWLEDGEMENTS.....	iii
LIST OF TABLES.....	v
LIST OF FIGURES.....	vi
INTRODUCTION.....	1
Importance of the Study.....	6
Study Objectives.....	7
Study Period and Study Area.....	8
DATA SOURCES AND DESCRIPTION.....	9
SSM/I Description.....	9
METHODS.....	13
Temporal Response of frozen land.....	13
Linear Association among the frozen land duration, air temperature and GPP....	16
RESULTS AND DISCUSSION.....	20
Temporal Analysis.....	20
Correlation Analysis.....	24
Graphical Analysis.....	29
CONCLUSIONS.....	34
FUTURE WORK RECOMMENDATIONS.....	36
REFERENCES.....	37
GLOSSARY.....	40
APPENDIX.....	41

## LIST OF TABLES

---

<b>Table 1.</b> Spatial resolution of four channels on SSM/I Sensor.....	9
<b>Table 2.</b> Identification number assigned to the pixels belonging to different categories of the land surface condition.....	11
<b>Table 3.</b> Classifying the frozen land depending on the duration of the land in the frozen state.....	19
<b>Table 4.</b> Chi-Square Values for frozen pixels of North America and Northern Eurasia..	21
<b>Table 5.</b> The change in frozen land area (million sq. km) from the preceding month in each event during freezing and thawing periods of North America and Northern Eurasia.....	23
<b>Table 6.</b> The correlation coefficient, $r$ , among the average frozen land duration, average air temperature and average GPP .....	28
<b>Table 7.</b> The descriptive statistics of frozen land, air temperature and GPP for all frozen land duration classes in North America.....	32
<b>Table 8.</b> The descriptive statistics of frozen land, air temperature and GPP for all frozen land duration classes in Northern Eurasia.....	33

## LIST OF FIGURES

---

<b>Figure 1.</b> Graphical representation of the El Niños and La Niñas events from 1950 to 2005 predicted by NOAA using MEI.....	2
<b>Figure 2.</b> A map showing the spatial variation of average temperature per a unit change in MEI from 1982-2000.....	3
<b>Figure 3.</b> The four possible phases and duration of land surface conditions that occur due to freeze thaw transitions in the northern high latitudes.....	4
<b>Figure 4.</b> Snow and Ice cover in Northern hemisphere.....	6
<b>Figure 5.</b> The area of study.....	8
<b>Figure 6.</b> Monthly Average Frozen Land Area (sq km) of North America and Northern Eurasia during the 1988-89 La Niña and 1997-98 El Niño events.....	20
<b>Figure 7.</b> Correlation analysis for three attributes describing North America.....	25
<b>Figure 8.</b> Correlation analysis for three attributes describing Northern Eurasia.....	27
<b>Figure 9.</b> The high-low bars plotted between frozen land duration and air temperature as well as GPP in North America.....	30
<b>Figure 10.</b> The high-low bars plotted against frozen land duration and air temperature as well as GPP in Northern Eurasia.....	31

## INTRODUCTION

The large-scale fluctuations in the Pacific Ocean's surface temperature and sea level pressure are termed El Niño and La Niña events. El Niño and La Niña are considered the major climatic events that disrupt the global climatic and weather conditions (Webster, et al. 1997). One of the most important parameters of climate is air temperature (Langenberg. 2002). Large-scale fluctuations in the atmospheric circulations that affect air temperature can also be associated with these events (Diaz, et al. 2000). The interaction between the land and the atmosphere causes the variation in the ground temperature that in turn affects the water content in the soil, leading to freezing and thawing of the land surface (Zhang, et al. 1999). The transition between freezing and thawing affects plant growth (Running, et al. 1999a).

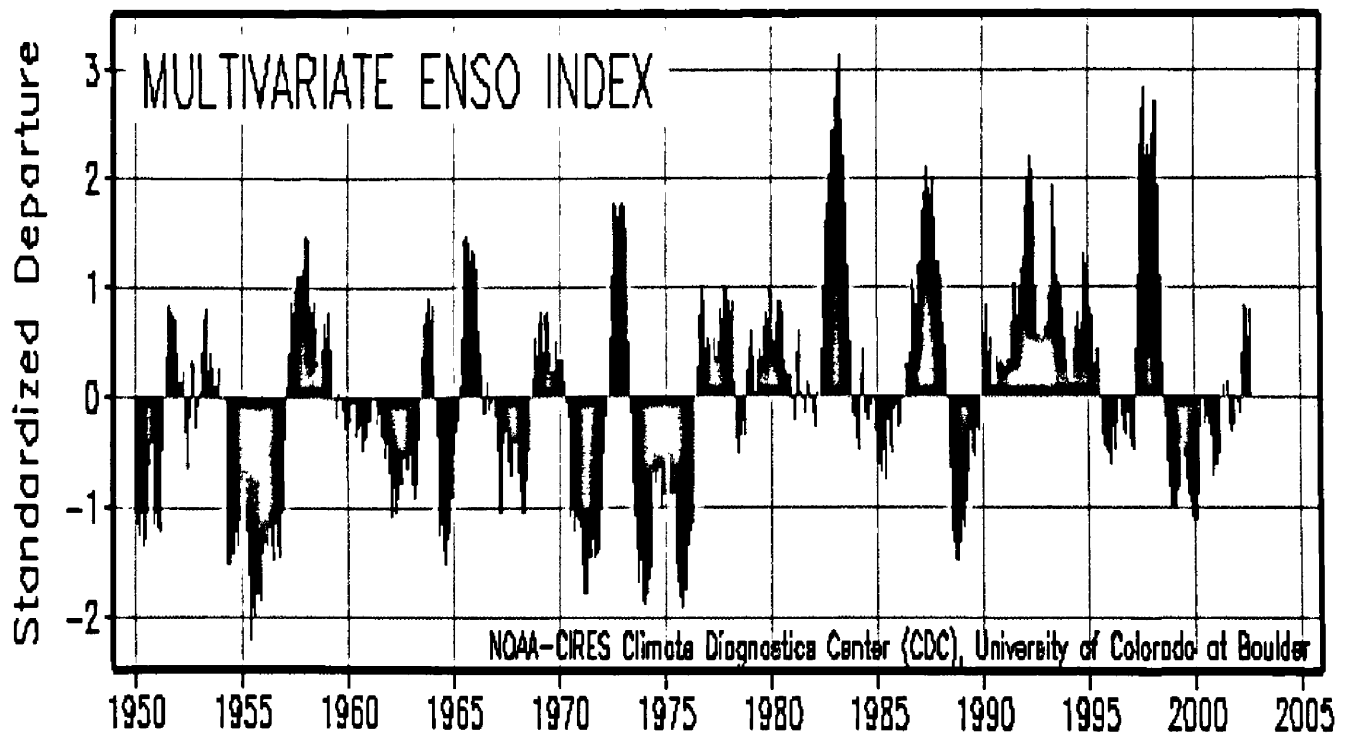
El Niño and La Niña events occur in the east-central Pacific Ocean and their influence spread across the globe. The degree of disruption varies spatially and temporally and differs for both events. The warming or cooling of Sea Surface Temperature (SST) by approximately 2 °C to 5 °C for at least four consecutive months is defined as an El Niño event and a La Niña event respectively (Trenberth, 1997). These events occur every 3 to 7 successive years, and are as labeled as weak, moderate and strong episodes depending on the duration. A strong El Niño or a strong La Niña event lasts for one to one and a half years.

These events bring extreme and opposite variations in oceanic temperature and pressure, in turn causing large scale changes in atmospheric temperature and pressure. The east-west atmospheric-pressure seesaw caused by these events is called as the Southern Oscillation (SO) (Neelin, et al. 1998). This coupled atmospheric and oceanic interaction that occurs in the core region of the tropical and the sub-tropical Pacific to Indian Oceans is termed as El Niño and Southern Oscillation (ENSO).

The Southern Oscillation Index (SOI) is one measure of the large-scale fluctuations in air pressure occurring between the western and eastern Pacific Ocean during El Niño and La Niña events (Harrison, et al. 2002). The SOI, the most traditional and conventional method of measuring El Niño and La Niña events, considers only the air pressure variation. The Multivariate ENSO Index (MEI) is another conventional way of describing the fluctuations in the ocean-atmospheric temperature and pressure over the tropical Pacific Ocean (Wolter, et al. 2002).

Unlike SOI, the MEI considers six variables to describe these variations (Wolter, et al. 1993): sea level pressure, zonal component of surface wind, meridional component of surface wind, sea surface temperature, land surface air temperature, and total cloudiness fraction over the globe. The list of El Niño and La Niña events from 1950 to 2005 as predicted by National oceanic Atmospheric Administration (NOAA) using MEI is shown in the following Figure 1.

**Figure 1. Graphical representation of the El Niños and La Niñas events from 1950 to 2005 predicted by NOAA using MEI**



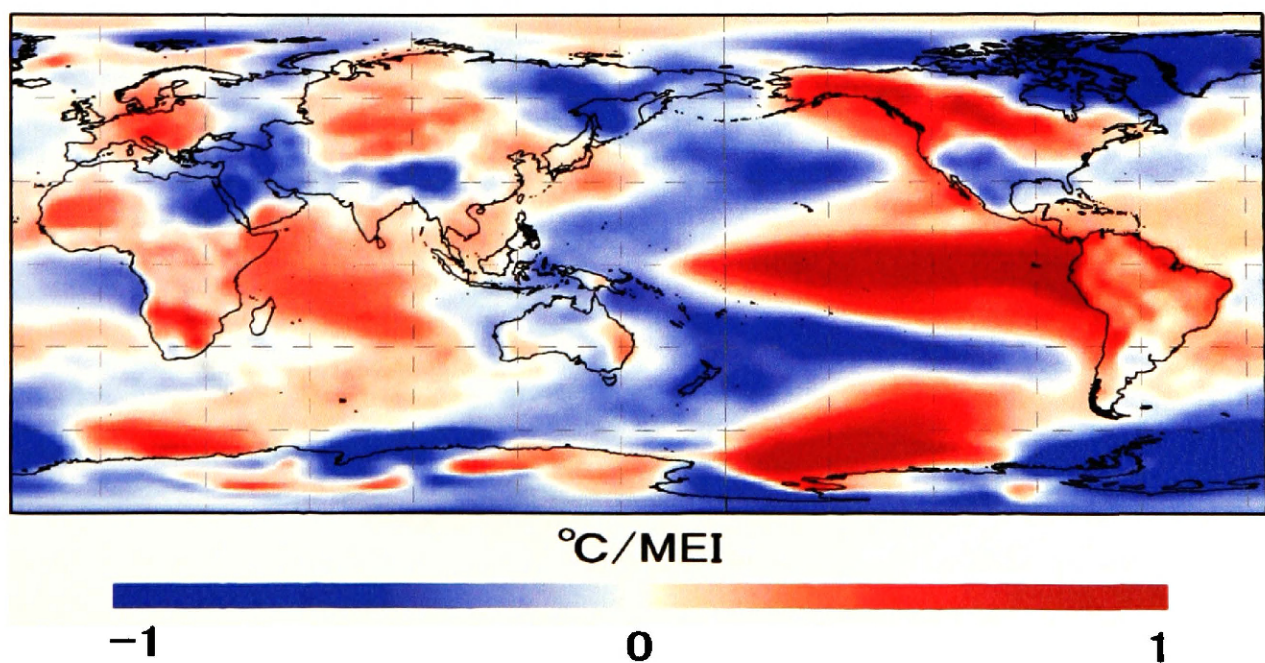


A negative value of MEI is considered to be a cold ENSO phase (La Niña) and a positive value of MEI is termed a warm ENSO phase (El Niño). The 1997-98 El Niño lasted for seventeen months, which started in the month of January 1997 and ended in the month of May 1998 (Slingo, 1998 and Wolter, et al. 1998) whereas the 1988-89 La Niña lasted for thirteen months, starting form May 1988 to June 1989 (Trenberth, 1997).

These oceanic and atmospheric interactions in the tropical Pacific region have a strong influence on global heat and water vapor transport and thus constitute an important component of climate (Pierrehumbert, et al. 2000 and Visser, et al. 2003). The effect on average air temperature due to a unit variation in MEI is shown in Figure 2. The figure demonstrates that an increase or decrease in the average air temperature is caused by a point increase or decrease in MEI respectively. This spatial variation in temperature is highly variable throughout the world (land/ocean). This map was developed by calculating the slope of each pixel when monthly average air temperature and monthly MEI are regressed against each other from 1982 to 1999.

**Figure 2. A map showing the spatial variation of average temperature per a unit change in MEI from 1982-1999**

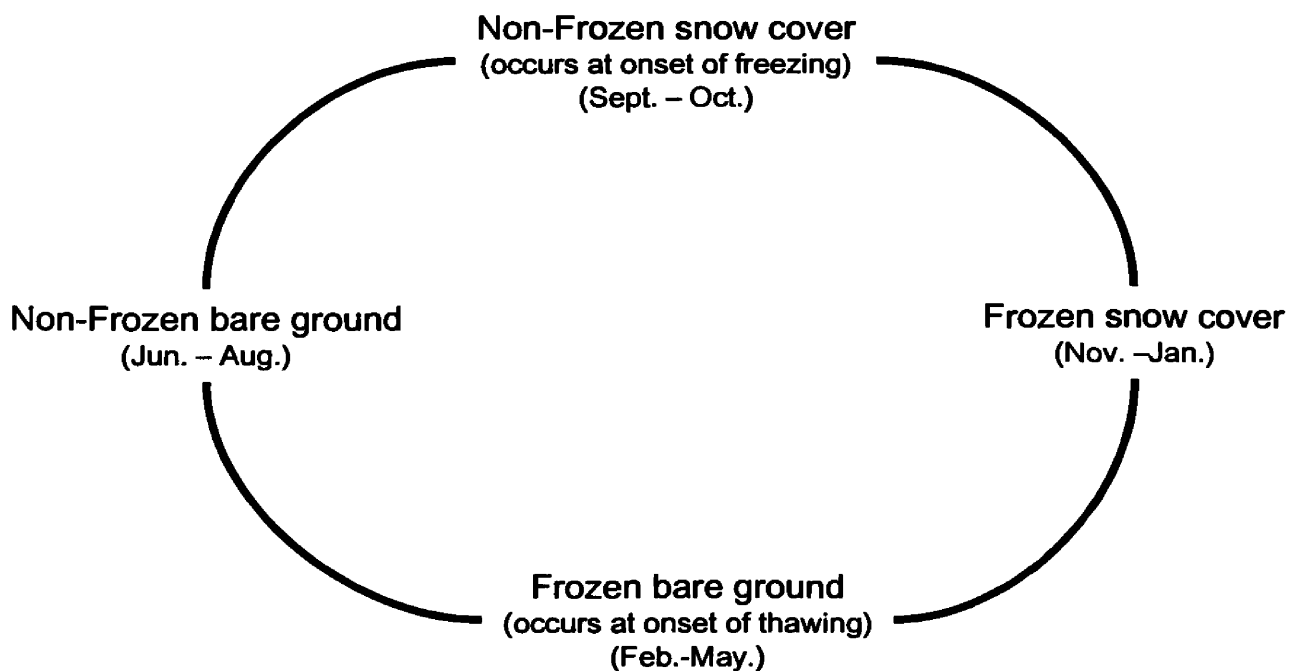
## Change of Average Temperature



Snow cover is the largest single component of the cryosphere about 98% of which is located in Northern Hemisphere (Armstrong, et al. 1999). Surface temperature is highly dependent on the presence or absence of snow cover (Armstrong, et al. 1999). When air temperature rises above freezing point (0° C), the surface soil temperature also reaches above 0° C. The fluctuation of temperature across the freezing point of water affects the water movement in soil (Hershfield, 1974). When the terrestrial air temperature and land surface temperature are above 0° C, the thawing of the surface starts, and when they are equal or below 0° C, freezing begins. Thus, Land surface temperature and air temperature influence the duration of the frozen and non-frozen states of land surfaces.

Freezing and thawing conditions are the frozen and non-frozen states of the land surface respectively. The freezing and thawing transitions in northern high latitudes occurs through four phases of land surfaces which are categorized as frozen bare ground, frozen snow cover, non-frozen bare ground and non-frozen snow cover (Figure 3).

**Figure 3. The four possible phases and duration of land surface conditions, that occurs due to freeze-thaw transitions in northern high latitudes**



$$\textit{Frozen Land} = \textit{Frozen Snow Cover} + \textit{Frozen Bare Ground}$$

The non-frozen snow cover land condition is possible by the onset of freezing period and frozen bare ground condition by the onset of thawing period. The non-frozen snow cover represents the ground covered by a thin layer of snow and the duration of it can be very short. The amount of non-frozen land cover is found to be negligible (Appendix Figure 3). The frozen snow cover, frozen bare ground and non-frozen bare ground land conditions constitute major phases of land surface conditions. Though the frozen bare ground is the beginning of thawing period, the amount of frozen land during this condition is huge and the ground will be in this phase for longer time i.e., a period between three to four months. Thus, frozen land is considered as frozen bare ground and frozen snow covered land.

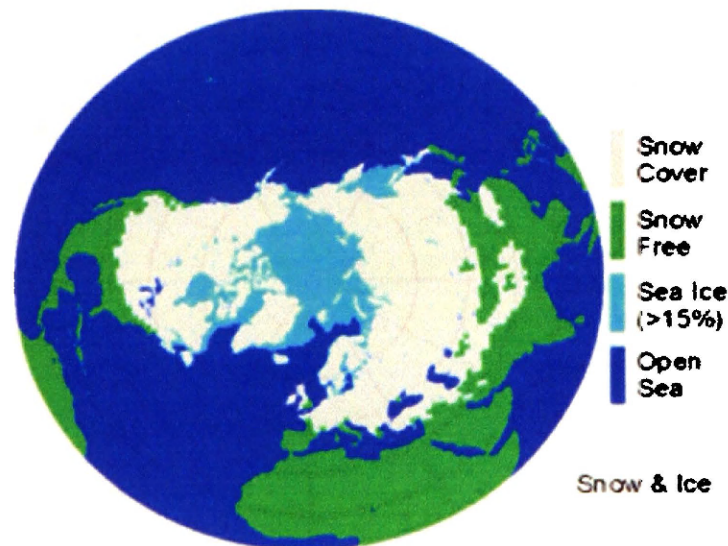
In a normal climatic year, other than El Niño or La Niña, land surface should freeze between the months of September and October and should thaw between the months of March and April. Depending on the climatic conditions, the transition between freezing and thawing of the land surfaces can be affected, i.e., will take place either earlier or later.

This seasonal transition causes high fluctuations in ground thermal conditions both temporally and spatially resulting variation in soil moisture content and soil temperature fluctuates. It also changes soil structure and regulates the availability of the nutrients in the soils (Running, et al. 1999a). The variation in the soil moisture content, nutrient levels and temperature play an important role in plant growth. The vegetation productivity or plant growth are measured in terms of Gross Primary Production (GPP) and usually measured in Kg C/m<sup>2</sup>/day. The importance of vegetation in global climate and biogeochemical studies is well recognized (Myneni, et al. 1997b). Since this study is funded by the National Oceanic Atmospheric Administration (NOAA), the NOAA scientists and climatologists are interested in the results for weather prediction as well as understanding the global carbon cycling.

## IMPORTANCE OF THE STUDY

The seasonal snow cover, the largest component of cryosphere, covers up to 33% of the earth's total land surface of which 98% is covered by Northern Hemisphere (Armstrong, et al. 1999) (Figure 4). Approximately 55-60% of the exposed land surface in Northern Hemisphere undergoes seasonal freezing and thawing (Varani, 2000). These seasonal transitions between freezing and thawing cycles regulate heat storage and heat transfer from the land surface to the atmosphere throughout the world (Zhang, et al. 1996). The amount of energy released or absorbed for this transition between freezing and thawing would be much higher (almost 80 times) than the amount of energy that is released or absorbed for the heating or cooling of water (Varani, 2000).

**Figure 4. Snow and Ice cover in Northern hemisphere**



The timing, duration, thickness and distribution of frozen soils are primarily controlled by heat exchange between the atmosphere and land surface (Varani, 2000). For any climatic conditions, the transition between freezing and thawing occurs. The extent to which El Niño and La Niña affects the duration and timing of freeze and thaw is unknown; yet this physical process has important consequences on soil and atmospheric moisture levels, as well as on biological activity (Kimball, et al 2001 and Myneni, et al 1997a).

## **STUDY OBJECTIVES**

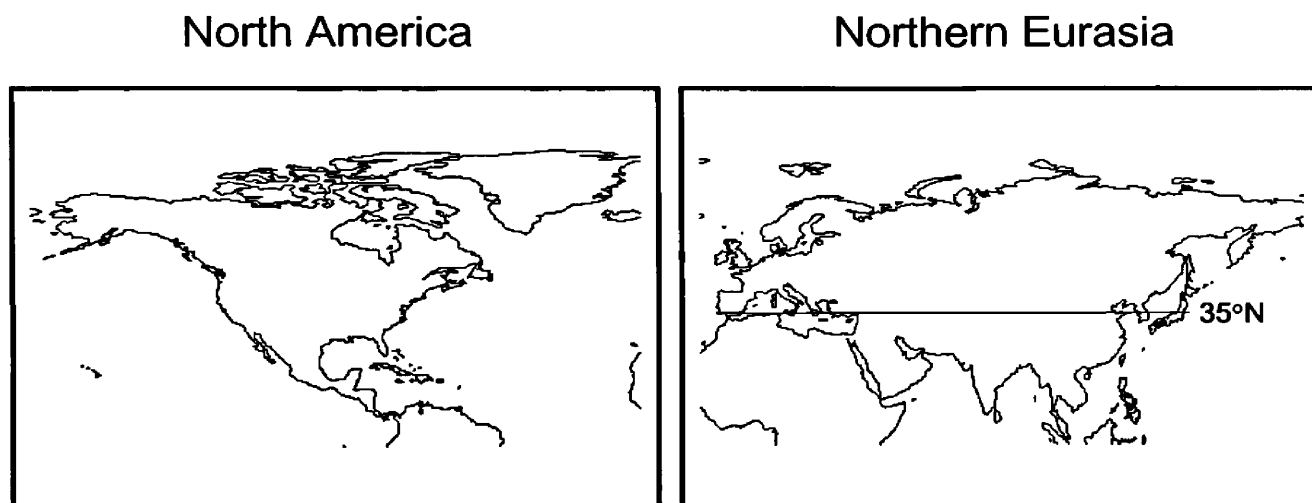
Thus, the objectives of this study are categorized into two.

- Describe the response of the seasonally frozen soils during the major climatic events (El Niño and La Niña)
- Describe the linear association between the frozen land duration and related climatic (terrestrial air temperature) and biophysical variables (Gross Primary Production, GPP).

## PERIOD AND AREA OF THE STUDY

There is the disruption of normal climate patterns at higher latitudes besides the shift in the major precipitation in the tropics due to El Niño or La Niña events (Webster, et al 1997). The datasets of freeze/thaw, air temperature and GPP are available for 1988-89 and 1997-1998 and coincidentally the most recent strong La Niña event and strong El Niño events occurred in 1988-1989 and 1997-1998 respectively (Figure 1). Since Northern Hemisphere is a huge land mass and the effect of ENSO is not the same within Northern Hemisphere (Figure 2). North Hemisphere is again sub-divided into Northern Eurasia [ $-15^{\circ}$  W to  $+180^{\circ}$  E and  $35^{\circ}$  N to  $90^{\circ}$  N], and North America [ $-172.5^{\circ}$  W to  $-14.5^{\circ}$  W and  $10^{\circ}$  N to  $90^{\circ}$  N] (Figure 5).

**Figure 5. The area of study**



Since, the effect of ENSO is significant in North America and not much on Eurasia, entire North America is considered in this study. Reason for considering only Northern Eurasia but not Eurasia is there is an abrupt transition occurs from frozen to thawed conditions occurs each year over roughly 50 million sq km of the Earth's remote terrestrial surface at latitudes above  $40^{\circ}$  N (Running, et al. 1999a).



## DATA SOURCES AND DESCRIPTION

The freeze-thaw data sets were acquired from the Defense Meteorological Satellite Program (DMSP) Special Sensor Microwave/Imager (SSM/I) through the National Snow and Ice Data Centers (NSIDC). The NSIDC is a part of the University of Colorado Cooperative Institute for Research in Environmental Sciences, and is affiliated with the National Oceanic and Atmospheric Administration (NOAA). It serves as one of the eight Distributed Active Archive Centers (DAAC) funded by National Aeronautics and Space Administration.

### SSM/I DESCRIPTION

The SSM/I is a sensor onboard the DMSP platform on the F-8 satellite launched in July 1987. Subsequent SSM/I's have been launched on the F-10, F-11, F-12, F-13, F-14, and F-15 satellites. Only the sensors on the F-13, F-14 and F-15 satellites are currently in operation. The SSM/I is a near-circular, sun-synchronous, polar-orbiting satellite at 860 Km above the surface of the earth with a 98.8 degrees inclination. The orbital period is 102 minutes and provides almost full coverage of the earth in one day. The SSM/I is a seven channel, four frequency (19.35, 22.235, 37, 85.5 GHz), passive microwave radiometric system which measures atmospheric, ocean and terrain microwave brightness temperature at the four different frequencies. Spatial resolution is different for each channel (Table1). All channels, except the channel at a frequency of 22.235 GHz, are dual-polarized. This means the sensor can transmit and receive signals in both horizontal and vertical directions of the same area.

**Table 1. Spatial resolution of four channels on SSM/I Sensor**

Frequency in GHz	Polarization	Spatial Resolution ( in Km)
19.35	V,H	49x69
22.235	V	40x60
37.0	V,H	29x37
85.5	V,H	13x15

Data collected by this sensor include various geophysical parameters such as rainfall rate, rainfall frequency, snow cover, and sea-ice, and is available on both daily and monthly time scales. Due to the ability of the microwave wave-length that can penetrate through clouds, provide data during day and night, and to provide an index of snow depth or water equivalent, passive microwave is a highly recommended satellite remote sensing technique to collect land surface freeze/thaw data (Armstrong, et al. 1999).

The SSM/I frozen soil algorithm (Judge, et al. 1996) is used to distinguish frozen pixels from non-frozen pixels in the freeze/thaw data. It requires two parameters: brightness temperature ( $T_B$ ) and spectral gradient ( $\delta T_B / \delta f$ ), where  $f$  is frequency of the signal. If the spectral gradient between 19 GHz and 37 GHz is negative and the brightness temperature at 37 V GHz is less than or equal to 258.2K a pixel is considered as frozen.

$$\delta T_B / \delta f \leq 0$$

$$T_B(37V) \leq 258.2$$

Since this soil algorithm cannot be used to distinguish snow-free soil from the snow-covered soil, the Goodison algorithm (Goodison, 1989) is used to identify the snow-covered land surface. The brightness temperatures of a pixel at 37 V GHz and 19 V GHz are substituted in the following expression.

$$GW = -2.74(T_B(37V) - T_B(19V)) - 20.7$$

Where, GW is an indicator and a value  $> 0$  implies the presence of snow on the ground surface.

Thus, the pixels are classified into non-frozen bare ground, frozen bare ground, non-frozen snow cover, frozen snow cover, missing, and ocean/lake. Missing data can be the pixels that are not identified using the SSM/I frozen soil algorithm and Goodison algorithm or it can be not captured by sensor for some reason such as operational failure of the sensor. A code is assigned to each class, and a detailed description and identification of the categories is given (Table 2).



**Table 2. Identification number assigned to the pixels belonging to different categories of the land surface condition**

Category	ID
Non-Frozen bare ground	1
Frozen bare ground	2
Non-Frozen snow cover	3
Frozen snow cover	4
Missing	7
Ocean/lake	8

Freeze/thaw datasets are available for each day starting from July 1, 1988 to June 30, 1989 as well as from July 1, 1997 to June 30, 1998. Daily global freeze/thaw datasets were created in the Equal Area Scalable Earth (EASE) (Appendix Figure 1) grid format at a 25 km by 25 km grid cell resolution by NSIDC (Armstrong, et al. 1995). Each data grid is composed of 721 rows and 721 columns. These data are available for the Northern Hemisphere.

Monthly average air temperature ( $^{\circ}\text{C}$ ) datasets were acquired from Legates and Willmott's (Peterson, T. C. 1997) which were in turn are collected from Global Historical Climatology Network (GHCN) stations. The GHCN is a comprehensive global surface baseline climate dataset designed to monitor and detect climate change. All GHCN datasets are available on a daily basis and are comprised of surface station observations of minimum, maximum and mean temperature, precipitation, and air pressure. These data are available via anonymous FTP from the National Climatic Data Center (NCDC) (Legates, et al. 1990a). The air temperature values from these stations are then spatially interpolated using a spherically-based interpolation algorithm (Legates, et al. 1990a) into a  $0.5^{\circ}$  latitude by  $0.5^{\circ}$  longitude grid to obtain the values for the entire world.

The daily average GPP data are calculated using MODIS MOD17 algorithm (Running, et al. 1999b) and these datasets were also used by Nemani in his Science paper published in 2003 (Nemani, et al. 2003). The MOD17 algorithm requires daily values of Fraction of Photosynthetically Active Radiation (FPAR), Photosynthetically Active Radiation (PAR), Vapor Pressure Deficit (VPD), and air Temperature (T) for deriving GPP. Using the NDVI values derived from NOAA Advanced Very High Resolution Radiometer (AVHRR), monthly average FPAR values had been calculated (Myneni, et al. 1997), and these values are then interpolated to obtain the daily average FPAR. Daily average air Temperature (T), Vapor Pressure Deficit (VPD), and PAR are obtained from the National Center for Environmental Prediction (NCEP) center. The range for the maximum radiation conversion efficiency ( $\epsilon_{\max}$ ) is (0.0006 – 0.0012) and it changes with the vegetation type. Thus, the daily average GPP (kg C/m<sup>2</sup>/day) is calculated using the MODIS MOD17 algorithm as:

$$\text{GPP} = \epsilon_{\max} * \text{FPAR} * \text{PAR},$$

Where,  $\epsilon$  is the conversion efficiency is the function of temperature and vapor pressure deficit and is calculated using the following expression

$$\epsilon = \epsilon_{\max} * f(T) * f(\text{VPD})$$

Daily average GPP data and monthly average air temperature data are available for 1988, 1989, 1997, and 1998 (four years) from January 1 to December 31. Each dataset consists of 720 rows by 360 columns, and is available globally. These data sets are in the Geographic Projection with a resolution of 0.5° x 0.5° latitude and longitude.

## METHODS

The objectives of this study are to describe the temporal response of the frozen and non-frozen soils due to the MEI variation and find a correlation on the related biophysical variable (GPP) during the 1997-98 El Niño and the 1988-89 La Niña events. The 1997-98 freeze/thaw data has only 352 days available starting from 1 July '97 to 19 June '98, though 1988-89 has data for the full year, i.e. 1 July '88 to 30 June '89. Hence, I have defined a year as from July to June, which has only 352 days only.

A transformation from the azimuthal Equal Area Scalable Earth grid (EASE) (Appendix Figure 1) projection with 25 km by 25 km grid size to Geographic grid projection (Appendix Figure 2) of  $0.5^\circ$  by  $0.5^\circ$  latitude/longitude was performed using an Interactive Data Language (IDL) program (Appendix Program 1) to compare freeze-thaw data with air temperature and GPP data sets. The study area i.e., North America and Northern Eurasia (Figure 5) are obtained from Northern Hemisphere depending on the array size. The array sizes of Northern Hemisphere, North America and Northern Eurasia are (712,712), (313,161) and (390,110) respectively. Freeze/thaw datasets contain six categories classified using the frozen soil algorithm and Goodison algorithm (Goodison, 1989 and Judge, et al. 1996). Depending on the land surface condition each category was assigned a code (Table 2).

### **Temporal Response:**

The temporal response of frozen land is studied by calculating the monthly area of frozen land and monthly Chi-square test values for both events in two regions. The Chi-square test values are only used to support the area analysis. As the study is about freezing and thawing of land surface, the ocean/lake and missing pixels are eliminated from all data sets (freeze/thaw, air temperature and GPP). It is also found that some of the missing pixels in 1997-98 are not missing in 1988-89 and vice versa. In order to avoid the incorrect conclusions, the missing pixels and ocean/lake pixels in both events are made as

one category and considered as missing data. The missing data for each day between the two years were checked and if they did not agree, those pixel values were classified as missing. The following code in IDL shows how this task was accomplished. Here dummy and dummy1 are float arrays consisting of two year data together in one file with 1997-98 year data from days 1-352 and 1988-89 year data from days 352-704. Dummy has array dimensions of (313,180,704) or (390,180,704) and dummy1 has dimensions of either (313,161,704) or (390,110,704).

```

if (dummy[i,j,k] eq 7) OR (dummy[i,j,(k+352)] eq 7) or (dummy[i,j,k] eq
8) OR (dummy[i,j,(k+352)] eq 8) then begin
    dummy1[i,j,k] = 5
    dummy1[i,j,k+352] = 5
endif else begin
    dummy1[i,j,k] = dummy[i,j,k]
    dummy1[i,j,k+352] = dummy[i,j,k+352]

```

The average number of pixels and the average area for non-frozen bare ground, non-frozen snow cover, frozen snow cover and frozen bare ground for each month in both years are calculated using the following program. The monthly average area (sq km) of the frozen land is obtained by multiplying the area of a pixel with the number of days the pixel is frozen. Here dummy1 and day\_cat are float arrays of sizes (313/390,161/110,30/31) and (313/390,161/110,5) respectively.

```

index1 = dummy1[i,j,*] eq 1
n1 = total(index1)
day_cat[i,j,0] = n1
.....
.....
index5 = dummy1[i,j,*] eq 5
n5 = total(index5)
day_cat[i,j,4] = n5

```

The monthly average number of pixels for a category

```

for i = 0,4 do begin ;i is the category
count_pixel[i] = total(day_cat[*,*,i])/30
endfor

```

The monthly average area (sq km) of the five categories

```
for i = 0,4 do begin
  month_area[i]=0.0
  for j=0,x do begin
    for k=0,y do begin
      month_area[i]=month_area[i]+(day_cat[j,k,i]*area[j,k])/30.00
    endfor
  endfor
endfor
```

The distribution of the frozen land between these events is checked using Chi-square test. A Chi-square test is chosen since the data (freeze/thaw) is a multinomial, i.e., data consists of counts of pixels in two states (frozen and non-frozen) assigned to two years (1997-98 and 1988-89). The monthly Chi-square values are obtained by using the monthly observed and expected values (Appendix Chi-square Method). The monthly-observed values are the monthly average number of pixels calculated using the IDL code above.

The freezing and thawing of land surface condition will be known by the amount of increase or decrease in frozen land only frozen bare ground and frozen snow covered land categories are used from here onwards. Because the land surface can be either frozen or non-frozen, the increase in frozen land should be a decrease in non-frozen land and vice-versa. Thus, the increase or decrease of only frozen land is analyzed. The frozen land/pixel is considered as frozen bare ground and frozen snow cover.

A freezing period is defined from the month of August to the month of November and a thawing period from the month February to the month of May (Figure 3). The shift in transition, if there is any, between freezing and thawing will be known from the amount of increase and decrease in frozen land area during freezing and thawing period. Thus, the difference between the area of frozen land between preceding months in both periods

is calculated to find the rate of change in amount of frozen land area from which the timing of the freezing/thawing in each event can be known.

**Linear association between the duration of frozen land, air temperature and GPP:**

The linear associations among the duration of frozen land, air temperature and GPP are described by correlation coefficients and correlation graphs. The air temperature data and GPP data are extracted for North America and Northern Eurasia from the global data sets. The pixels in these data sets (air temperature and GPP) that represent missing pixels in the freeze/thaw data were eliminated. In order to do this, the maximum number of days in a year that a pixel is present in a specific category of freeze/thaw data is calculated using the following code (Appendix Program 4).

```

for i = 0,x do begin
  for j = 0,y do begin
    count[*] = 0L
    for k = 352,703 do begin
      if (dummy[i,j,k] eq 1) then begin
        count[0] = count[0]+1
      endif
      .....
      .....
      if (dummy[i,j,k] eq 4) then begin
        count[3] = count[3]+1
      endif
    endfor
    if (count[0] eq 0 AND count[1] eq 0 AND count[2] eq 0 AND count[3] eq 0) then
begin
      output[i,j] = 5
    endif
    if (count[0] gt count[1]) AND (count[0] gt count[2]) AND (count[0] gt count[3])
then begin
      output[i,j] = 1
    endif
    .....
    .....
    if (count[3] gt count[0]) AND (count[3] gt count[1]) AND (count[3] gt count[2])
then begin
      output[i,j] = 4
    endif
  endfor
endfor

```

```

        sum[*] = sum[*]+count[*]
    endfor
endfor

```

Once the maximum count of a pixel in a category of freeze/thaw data is known, the air temperature and GPP pixels that are found as missing in freeze/thaw data were eliminated by overlaying the freeze/thaw datasets with the air temperature and GPP data sets. The monthly average air temperature and monthly average GPP are obtained (Appendix Program 5 and 6). The code to overlay the air temperature data with the freeze/thaw data so as to eliminate the missing pixels in freeze/thaw data in air temperature data as well as calculating the monthly average air temperature is as follows:

```

for k = 0,11 do begin
    if (dummy1[i,j] ne 5) then begin
        temp2[i,j,k] = dummy[i,j,k]*area[i,j]
        sum[k]=sum[k]+area[i,j]
    endif
endfor

avet = fltarr(12)
for i = 0,11 do begin
    avet[i] = total(temp2[*,* ,i])/sum[i]
endfor

```

The code to overlay the GPP data with the freeze/thaw data to eliminate the missing GPP pixels in freeze/thaw data as well as calculating the monthly average GPP follows:

```

for k = 0,11 do begin
    if (table[i,j] ne 5) AND (B[k,i,j] gt 0) then begin
        dummy[k,i,j] = B[k,i,j]*area[i,j]
        sum[k]=sum[k]+area[i,j]
    endif
endfor

gpp_month=fltarr(12)
for i = 0,11 do begin
    gpp_month[i] = total(dummy[i,* ,*])/sum[i]
endfor

```

The correlation coefficient,  $r$ , and correlation graphs among the frozen land duration, air temperature and GPP for each event is obtained using the following code (Appendix Program 7).

```
dummy = ftarr(390,110,5) ;NA=(313,161,5)—here dummy is #of days a pixel is frozen
y = ftarr(390,110) ;air temperature
z = ftarr(390,110) ;GPP, Kg C/m2/month

z = z*1000
x = ftarr(390,110) ;frozen=frozen bare ground(1) and frozen snow cover(3)
x[*,*] = dummy[*,*],1]+dummy[*,*],3]
ind=where(y[*,*] ne 0.0 and y[*,*] ne -999.0 and z[*,*] ne -999.0)
plot, y[ind[*]], z[ind[*]], psym=1,symsize=0.5, color = 1
result = correlate(y[ind[*]],z[ind[*]])
```

The correlation coefficient as well as correlation graphs are used to interpret the general patterns of relation among these attributes (frozen land, air temperature and GPP). Though the correlation was always not strong between these attributes, a pattern appeared to exist depending on the frozen land duration. Hence, the frozen land pixels are classified into seven depending on the duration of the land (Table 3) to find the variation of air temperature as well as GPP with in each class. The air temperature and GPP data for each pixel under a specific class are obtained (Appendix Program 8). The code is written here under.

```
if (0 le x[i,j]) and (x[i,j] lt 49) and (dummy2[i,j] ne 0.0) and (dummy2[i,j] ne -
999.0) and (dummy3[i,j] ne -999.0) then begin
```

where,  $x$  is the data of frozen land duration,  $dummy2$  is air temperature data and  $dummy3$  is GPP data.



**Table 3. Classifying the frozen land depending on the duration of the land in the frozen state**

Duration of Frozen land	ID
0-49	1
50-99	2
100-149	3
150-199	4
200-249	5
250-299	6
300-352	7

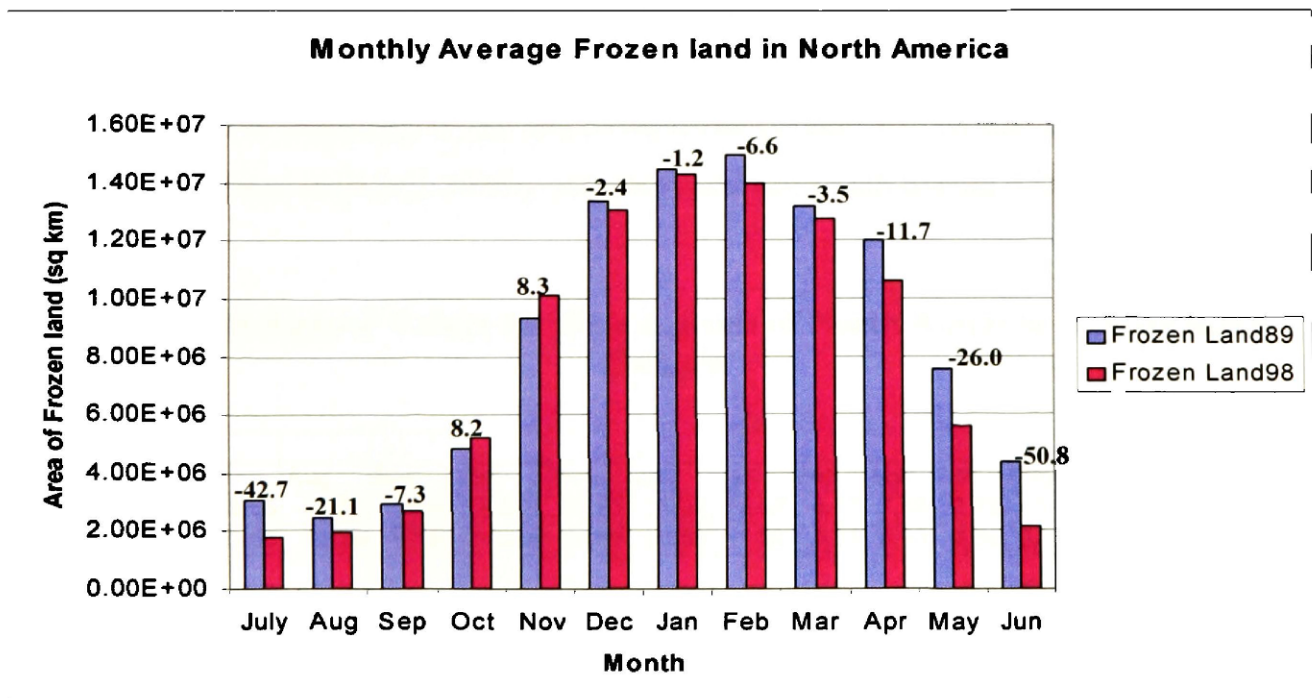
The class and three attributes are entered year wise in SPSS as columns, where classes and corresponding data for each class of three attributes are entered in the ascending order of classes. The descriptive statistics such as total number of pixels in each class (N), mean and standard deviation for the three attributes for all classes are obtained for both events and regions. The variations of the air temperature and GPP with in each class with respect to the duration of frozen land duration are found using the high-low bars plotted using SPSS. The high value is sum of one standard deviation and the mean whereas low value is the subtraction of one standard deviation from the mean. The close variable is chosen as the mean value of the respective attribute (air temp/GPP).

## RESULTS AND DISCUSSION

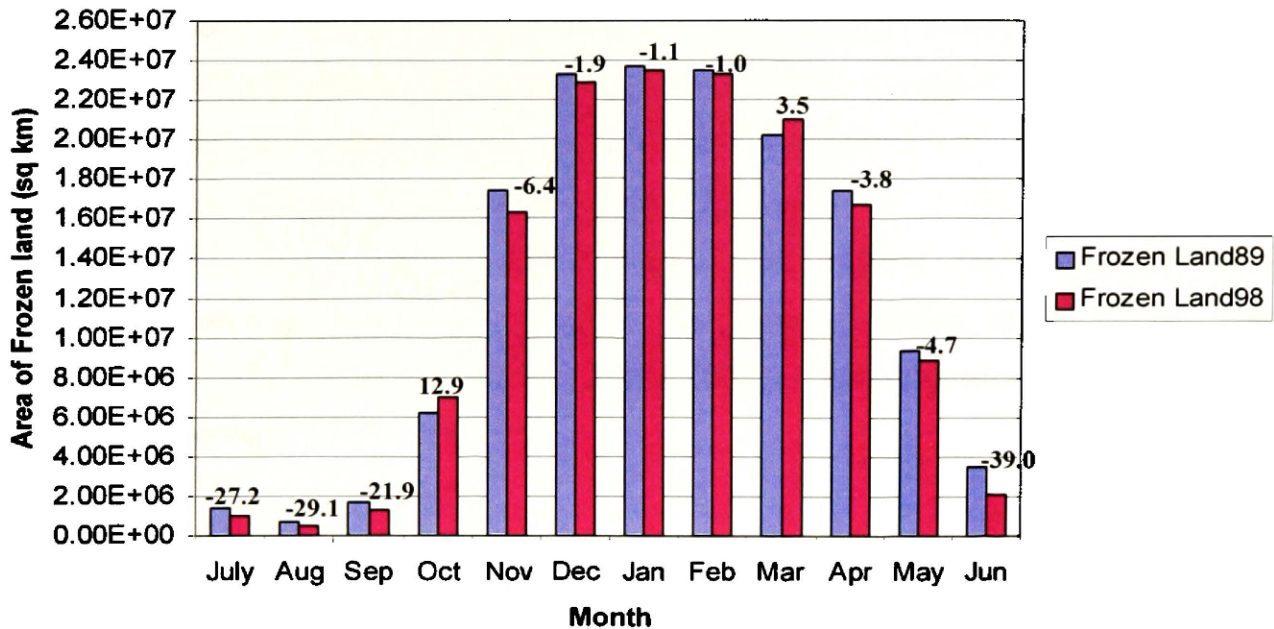
### Temporal Analysis:

The monthly average area of the frozen land (sq km) (Figure 6) as well as the monthly average number of frozen pixels obtained using chi-Square test (Table 4) shows that the temporal distribution of the amount of frozen land (area/number) is not the same between the two events for both regions. The greater difference in chi-square values and greater difference between frozen land area between two events for North America can be due to significant difference of frozen pixels in the months of May, June, July, October and November. However, there the chi-square values and frozen land area between events in Northern Eurasia is not same the difference in each month between the events is not much except for the months of June, July and November.

**Figure 6. Monthly Average Frozen Land Area (sq km) of North America and Northern Eurasia during the 1988-89 La Niña and 1997-98 El Niño events**



**Monthly Average Frozen land in Northern Eurasia**



The percent of increase or decrease in frozen land area between the events with 1988-89 as the base year is displayed at the top of each bar (Figure 6). Notice that there is a huge difference in frozen land area during summers and not much during winters.

**Table 4. Chi-Square Values for frozen pixels of North America and Northern Eurasia**

North America												
	Jul	Aug	Sep	Oct	Nov	Dec	Jan	Feb	Mar	Apr	May	Jun
1997-1998	93.68	14.52	1.912	23.622	37.92	11.69	13.03	4.17	7.58	0.73	40.68	238.32
1988-1989	85.68	13.28	1.749	21.606	34.68	10.69	11.92	3.81	6.93	0.66	37.21	217.98

Northern Eurasia												
	Jul	Aug	Sep	Oct	Nov	Dec	Jan	Feb	Mar	Apr	May	Jun
1997-1998	22.67	12.79	29.19	26.124	3.363	0.096	0.992	1.35	11.1	0.07	0.036	101.75
1988-1989	22.14	12.49	28.51	25.517	3.284	0.094	0.969	1.32	10.8	0.07	0.035	99.381

It is observed that during the 1997-98 El Niño event, the total average area that is frozen for North America is approximately  $7.8 \times 10^6$  sq km it is little higher than  $12.0 \times 10^6$  sq km

for Northern Eurasia. However, during the 1988-89 La Niña event, the total average frozen land area is around  $8.5 \times 10^6$  sq km for North America and  $12.3 \times 10^6$  for Northern Eurasia (Appendix – Table 1). There is a decrease in total average frozen land of approximately 0.7 million sq km in North America while it reduced approximately by 0.33 million sq km in Northern Eurasia from 1988-89 La Niña to 1997-98 El Niño. Since there were more number of El Niño events that occurred in the decade of 1990 (Trenberth, 1997), this decrease in frozen land in both regions can be explained as a direct relation between frozen land and El Niño years (Running, et al. 1999a). That means that an increase in the number of El Niño events leads to a decrease in the average amount of frozen land.

The change in frozen land area between the months is the amount of the land that freezes or thaws due to the transition between the land conditions that occur because of variation in climatic conditions. The amount of frozen area that increased or decreased was shown (Table 5). The freezing of North America during the 1997-98 started in the month of August, at least a month earlier than the 1988-89 and it continued to increase until the month of November (mid-fall). However, by end of freezing period (December), the rate of the frozen land for the 1988-89 increased and it had almost  $1.0 \times 10^6$  sq km more frozen land than the 1997-98. Thus, it can be explained that North America, during the 1988-89 had started freezing slowly initially but later on the rate of increase of the frozen land was high. While, during the 1997-98, North America started freezing a month earlier than the normal freezing period, and showed a gradual increase in the area of frozen land only until the month November.

The rate of freezing of the land in Northern Eurasia for both events started in the month of September and the rate of increase of freezing is higher for the 1988-89 for the entire freezing period except for the month of November. In the month of November, the increase in the frozen land during the 1988-89 is approximately  $2.0 \times 10^6$  sq km higher

than during the 1997-98 (Table 5). Hence for Northern Eurasia, frozen land rapidly increased from September to November during 1997-98 and 1988-89.

On the other hand, thawing occurred from the month of February and the pattern of decreasing frozen land is similar for both events in both regions (Table 5). The rate of thawing for North America during the 1997-98 is gradually increasing and by the end of thawing period, it thawed at a rate of two to three times higher than the beginning. However, during the 1988-89, it thawed one month later than during the 1997-98 and it was rapid in the month of March, i.e., by the middle of the thawing period, and later on it decreased in April and again increased twofold from the beginning of May. In Northern Eurasia though the thawing started at the same time, in the month of February, for both events and the rate at which land thawed was rapid for the 1988-89 La Niña and it was gradual and fluctuating for the 1997-98. Overall, North American land as well as Northern Eurasian land thawed more in the 1997-98 than the 1988-89.

**Table 5. The change in frozen land area (million sq. km) from preceding months in each event during freezing and thawing periods for North America and Northern Eurasia.**

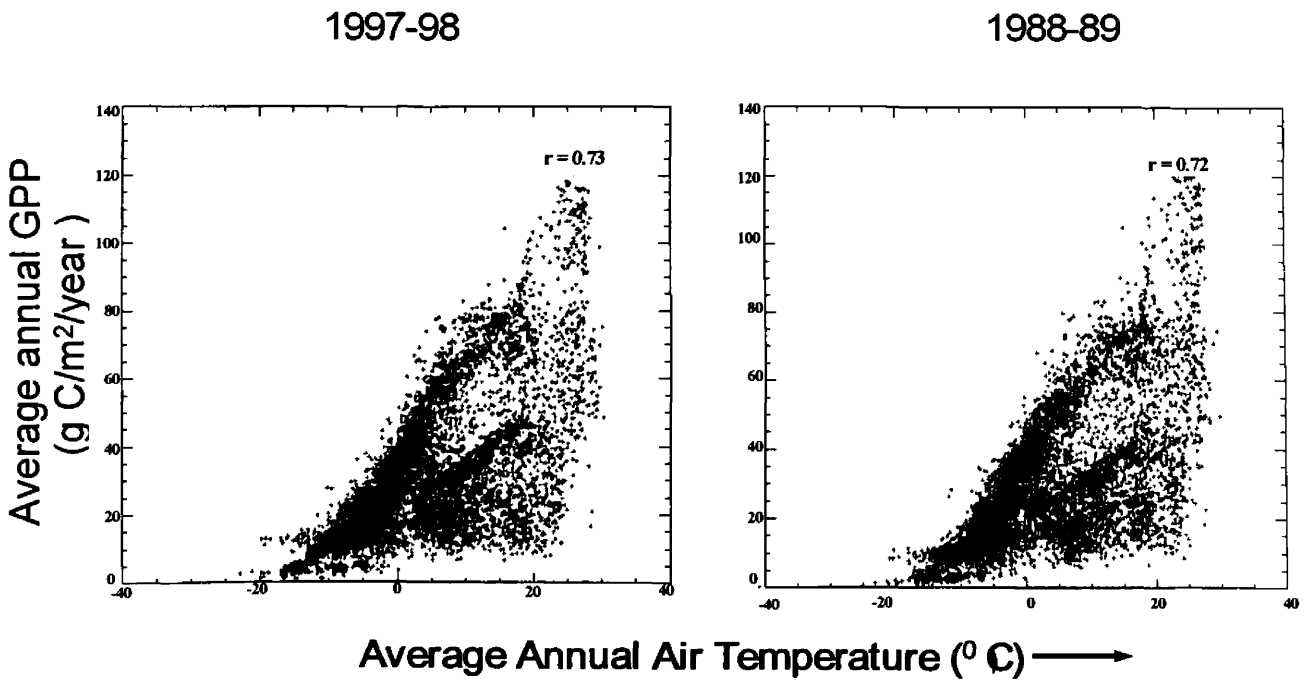
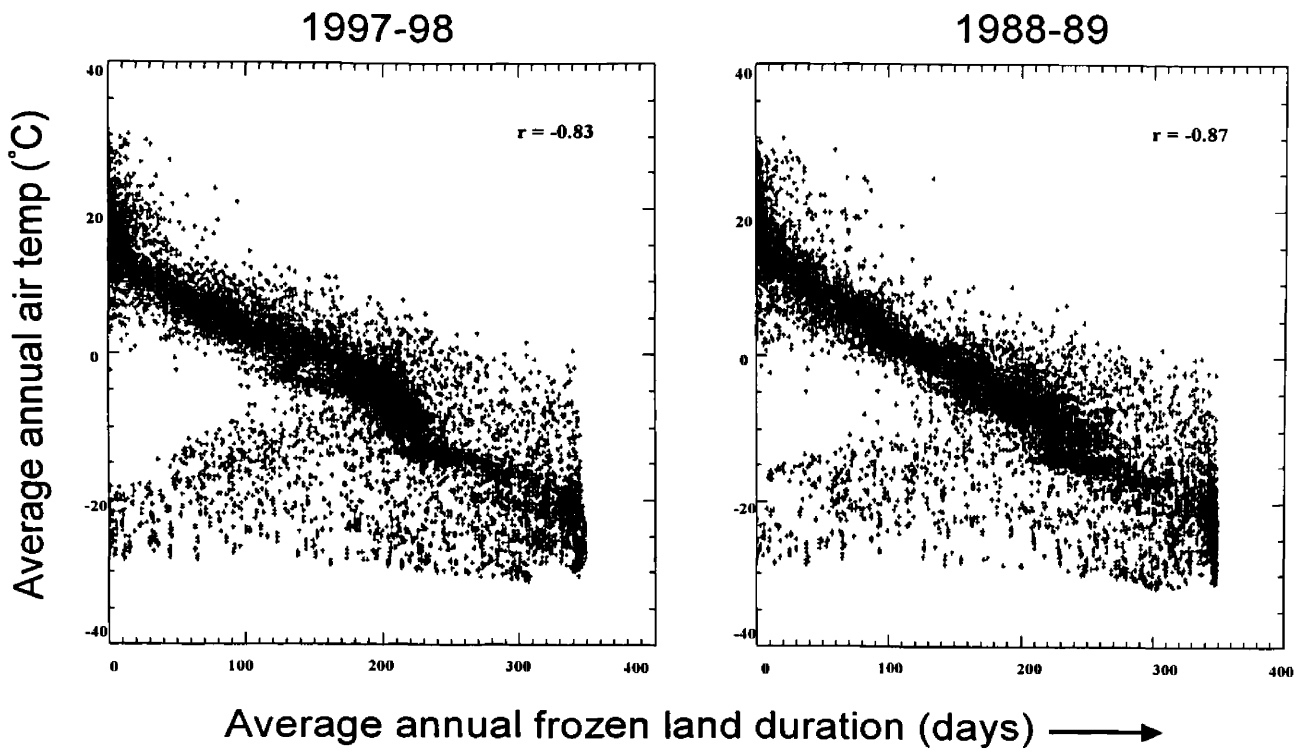
	Month	NA98	NA89	NE98	NE89
Freezing Period	(Aug-Jul)	0.19	-0.59	-0.48	-0.63
	(Sep-Aug)	0.76	0.45	0.79	0.95
	(Oct-Sep)	2.53	1.92	5.68	4.52
	(Nov-Oct)	4.85	4.47	9.37	11.28
	(Dec-Nov)	2.95	4.05	6.53	5.85
Thawing Period	(Feb-Jan)	-0.31	0.50	-0.20	-0.21
	(Mar-Feb)	-1.23	-1.75	-2.33	-3.29
	(Apr-Mar)	-2.12	-1.18	-4.24	-2.87
	(May-Apr)	-5.04	-4.49	-7.83	-8.04

### **Correlation Analysis:**

Correlation analysis was performed among three attributes taken two at a time (Figure 7 and 8). The relation between duration of the frozen land and average air temperature is negatively correlated and it is concentrated with a slight shadow effect for North America whereas it is strongly concentrated for the Northern Eurasian region. On the other hand, the relation between average air temperature and GPP is positively correlated and the relation between duration of the frozen land and average GPP is negatively correlated. But the pattern between the duration of frozen land and average air temperature as well as duration of frozen land and average GPP appear to be more or less random or dispersed for North America as well as Northern Eurasia.

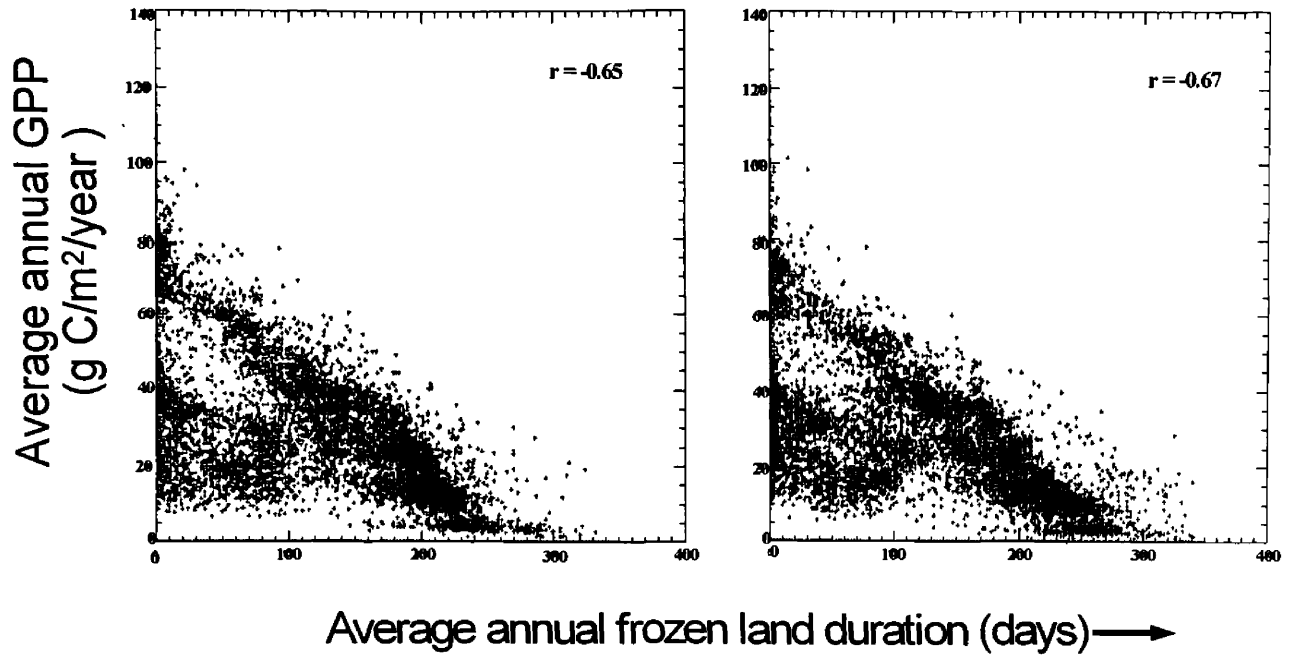
When observed closely, the correlation graph between frozen land duration and GPP as well as air temperature and GPP shows linear association. Though they are not highly correlated, the pixels in the graph seem to follow two individual patterns that had shown the linear association. There is no significant trend seen between the association of these attributes in Northern Eurasia except for the average duration of frozen land and average air temperature (Figure 7). The correlation coefficients,  $r$ , between the attributes are given in Table for North America and Northern Eurasia (Table 6).

**Figure 7. Correlation analysis for three climatic attributes describing North America**



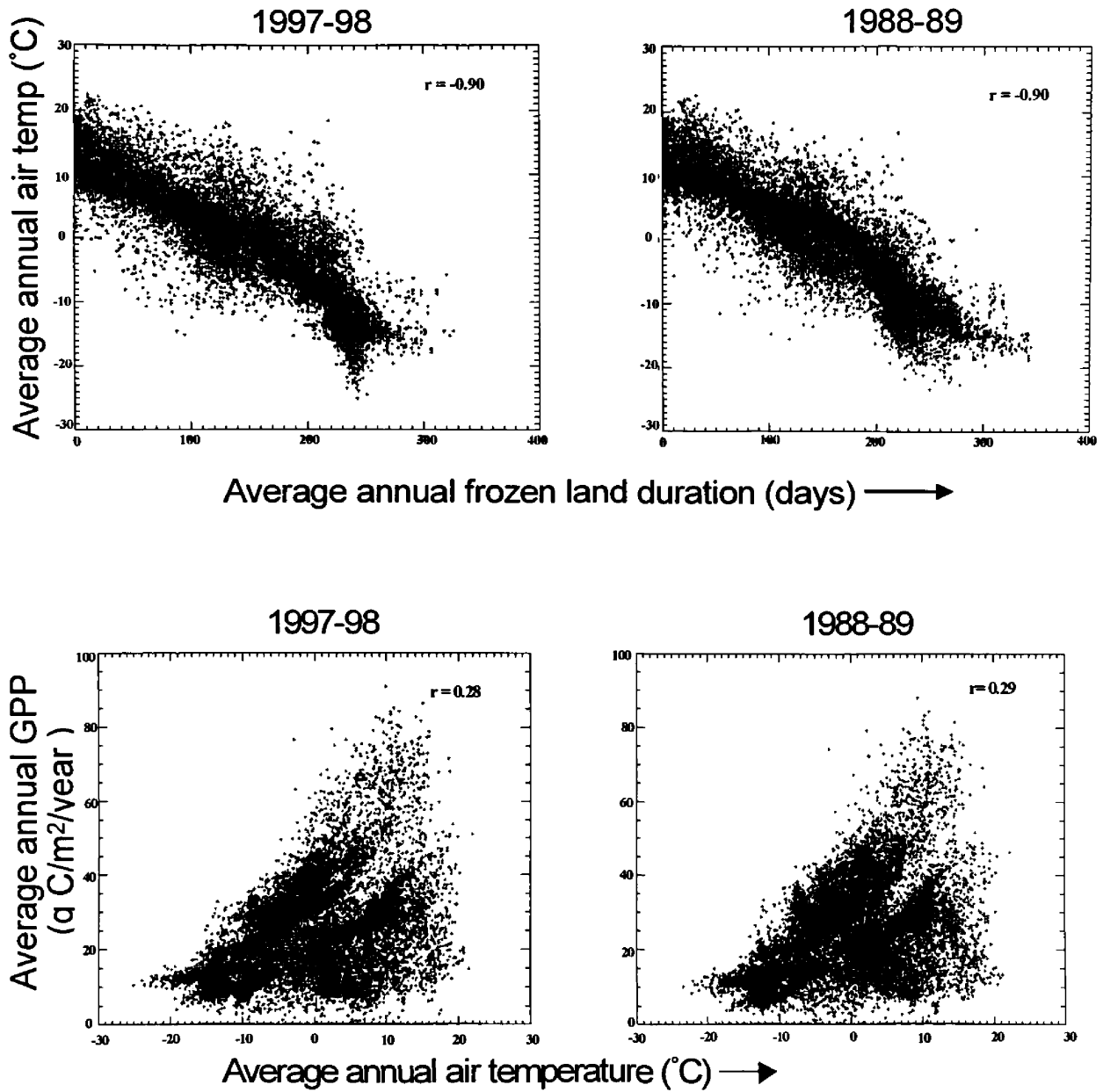
1997-98

1988-89





**Figure 8. Correlation analysis for three climatic attributes describing Northern Eurasia**



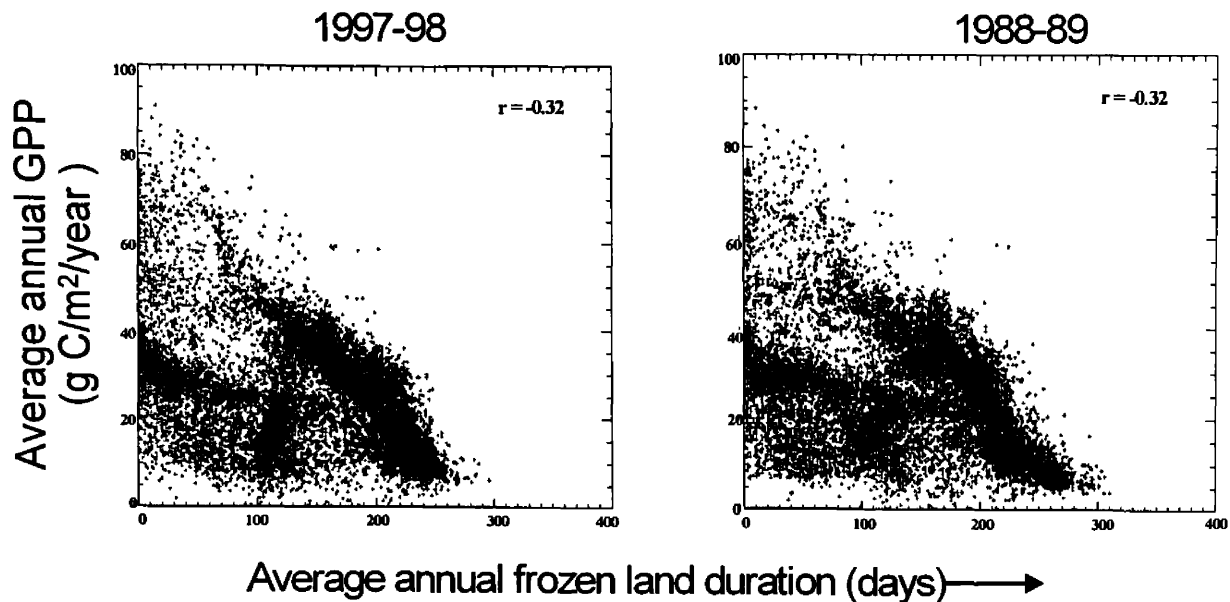


**Table 6. The correlation coefficient  $r$ , among the average frozen land duration, average air temperature and average GPP.**

Correlation Coefficient, $r$	NA98	NA89	NE98	NE89
average frozen land duration Vs average air temperature	-0.83	-0.87	-0.90	-0.90
average air temperature Vs average GPP	0.73	0.73	0.28	0.29
average frozen land duration Vs average GPP	-0.65	-0.67	-0.32	-0.32

### **Graphical Analysis:**

The correlation diagrams which are scattered, exhibit a lot of variation along the duration of frozen land, so High-Low bar graphs were created to further examine the nature of variation of air temperature and GPP with respect to each class of frozen land duration. Here the Y-axis is either air temperature or GPP and X-axis is always classes of frozen land duration.

For North America, the variation in air temperature with in each class of frozen land duration is the same for the first two and last two classes of the 1997-98 and the 1988-89. However, the variation with in each class is pretty but similar for all classes for the 1997-98 and not for the 1988-89. The average air temperature decreased along with the duration of frozen land (Figure 9). The variation of the GPP with in each class and average GPP is found to be higher and kept fluctuating for the first four classes of frozen land duration and decreased for rest of classes for both events.

On the other hand, for Northern Eurasia, the variation of air temperature is similar for the first four classes of frozen land duration and fluctuated for rest of the classes during the 1997-98 and the 1988-89. While the average air temperature decreased with the frozen land duration classes for both events. The GPP had higher variation and the average GPP kept fluctuating for first four classes of frozen land duration and then the variation with the class and the average GPP decreased for rest of the classes for both the years (Figure 10).

**Figure 9. The standard high-low bars plotted between frozen land and average air temperature as well as average GPP in North America**

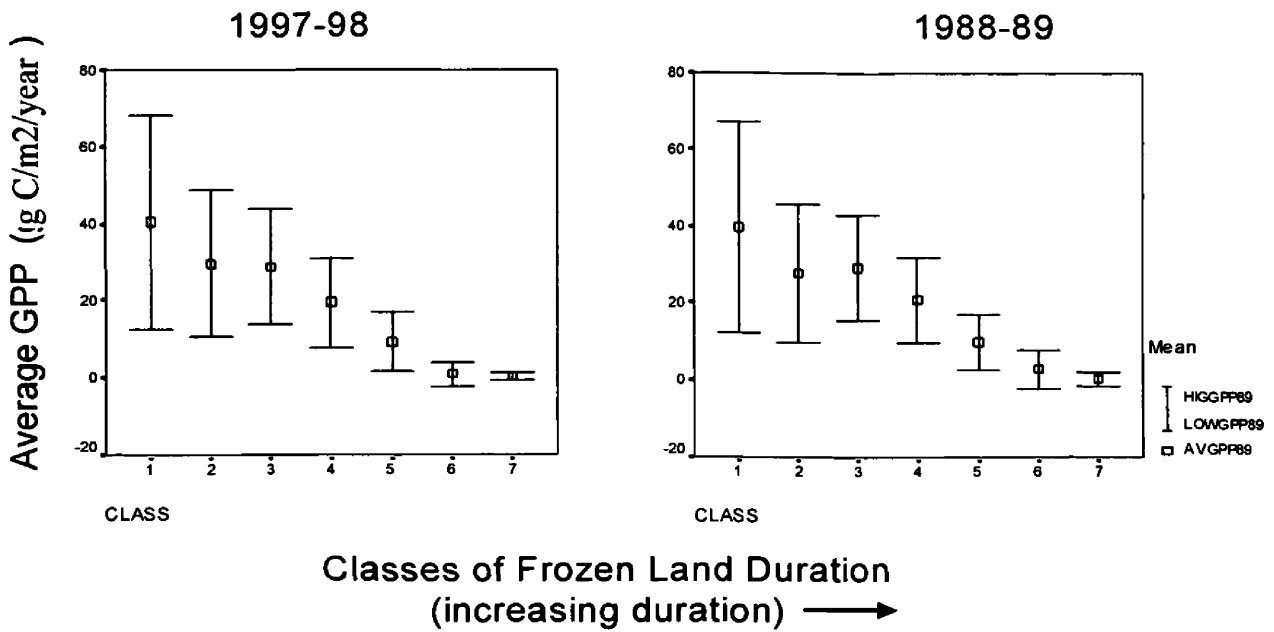
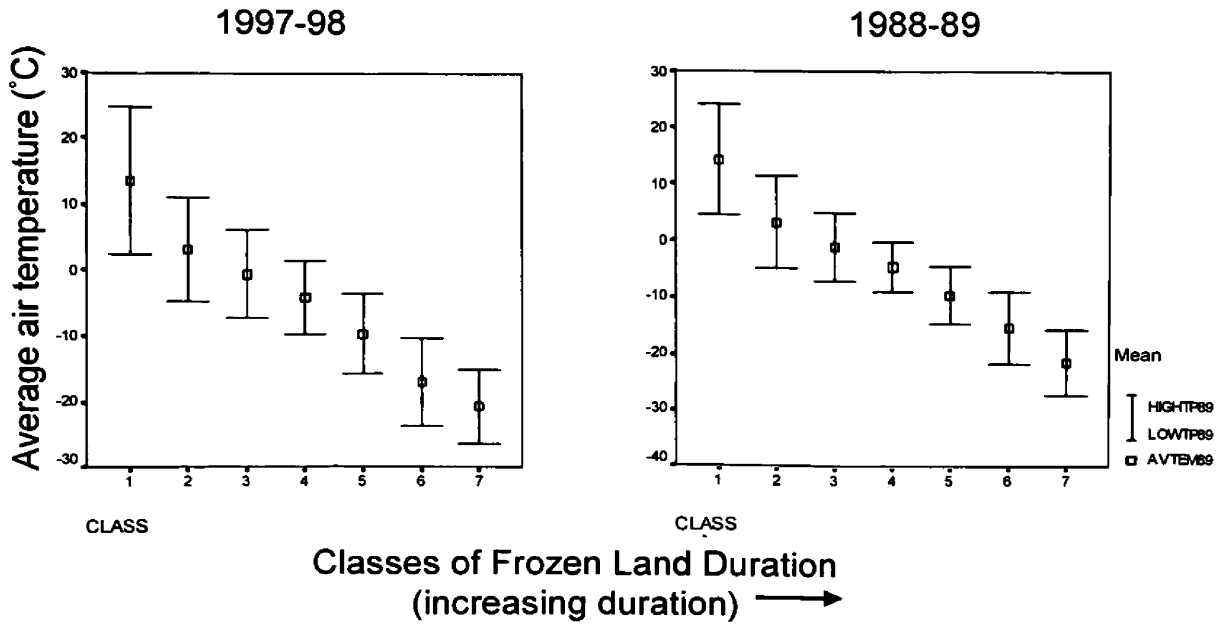
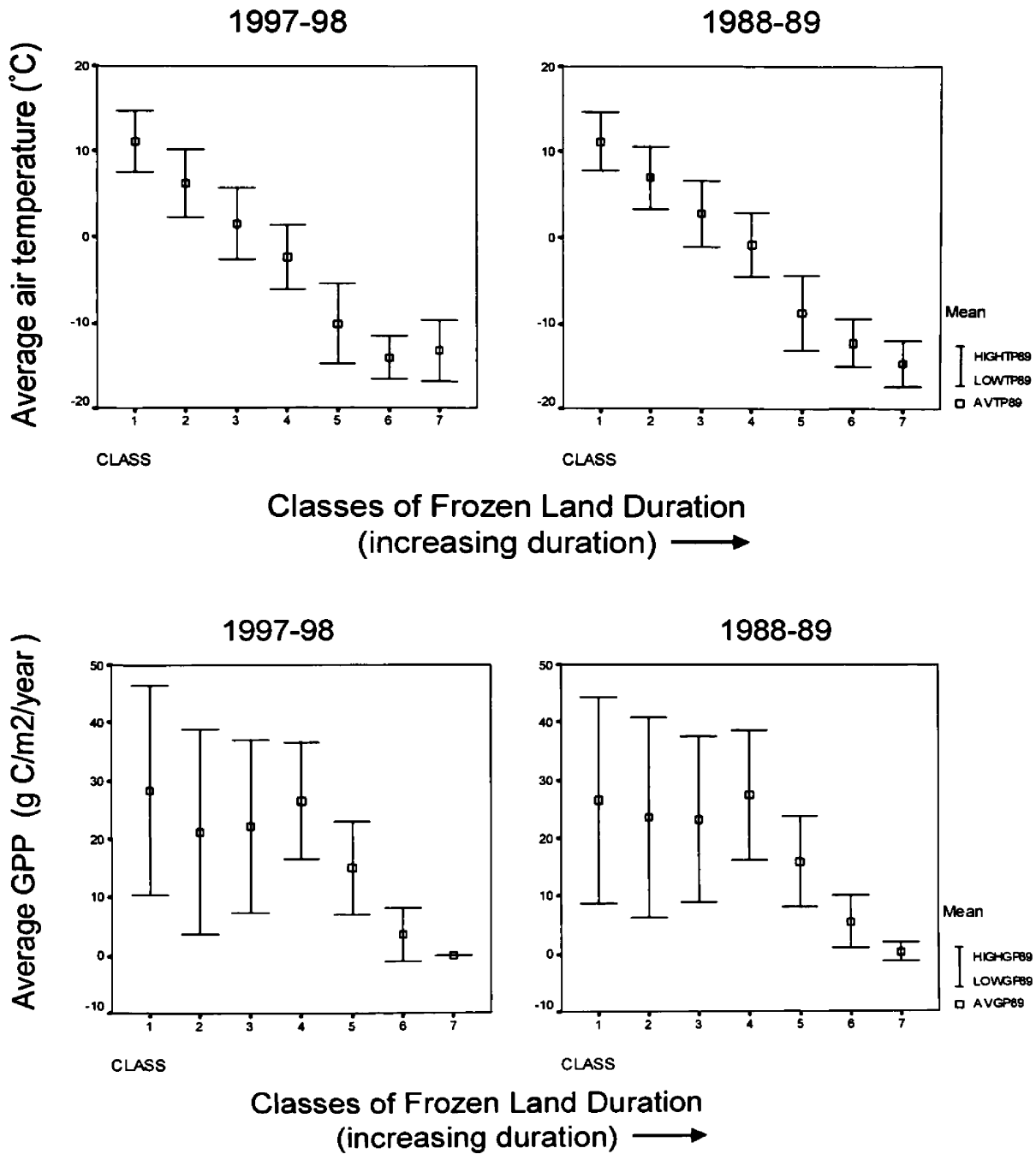


**Figure 10. The standard high-low bars plotted against frozen land and average air temperature as well as average GPP in Northern Eurasia**



The descriptive statistics, used to obtain the high-low graphs, shows that for North America, the total number pixels (N) that are frozen is higher from class 1 to class 5 of frozen land duration during the 1997-98 than the 1988-89 (Table 7). That means during the 1997-98 El Niño event, there was more number of pixels that are frozen whereas, for

the 1988-89 La Niña event, the pixels are frozen for longer duration of time. On the other hand, the number of pixels (N) that are frozen in each class kept fluctuating between the two events of Northern Eurasia (Table 8).

**Table 7. The descriptive statistics of frozen land, air temperature and GPP for all frozen land duration classes in North America**

Frozen land duration class	Total number of pixels (N)	Mean FL98	Mean Temp98	SD Temp98	Mean GPP98	SD GPP98
class1	3347	12.02	13.54	11.13	40.32	27.91
class2	1827	75.06	3.19	7.96	29.4	19.03
class3	1780	124.91	-0.56	6.65	28.57	14.95
class4	2324	178.14	-4.21	5.61	19.3	11.5
class5	2636	219.71	-9.69	6.1	9.25	7.82
class6	995	275.31	-17.1	6.8	0.89	3.07
class7	1410	327.15	-20.74	5.68	0.074	0.98

Frozen land duration class	Total number of pixels (N)	Mean FL89	Mean Temp89	SD Temp89	Mean GPP89	SD GPP89
class1	3235	13.86	14.22	9.68	39.76	27.49
class2	1616	76.97	3.16	8.24	27.55	17.92
class3	1516	124.03	-1.07	6.02	29.11	13.61
class4	2107	175.73	-4.56	4.4	20.69	11.08
class5	2495	223.51	-9.56	5.02	9.82	7.33
class6	1384	271.56	-15.27	6.41	2.86	4.84
class7	1966	334.71	-21.5	5.86	0.22	1.73

**Table 8. The descriptive statistics of frozen land, air temperature and GPP for all frozen land duration classes in Northern Eurasia**

Frozen land duration class	Total number of pixels (N)	Mean FL98	Mean Temp98	SD Temp98	Mean GPP98	SD GPP98
class1	3642	21.64	11.1	3.61	28.44	17.99
class2	2546	73.91	6.27	3.96	21.28	17.61
class3	3935	123.26	1.49	4.16	22.26	14.79
class4	3671	175.76	-2.41	3.74	26.61	10.08
class5	5413	224.43	-10.18	4.69	15.08	7.94
class6	605	262.18	-14.12	2.39	3.55	4.53
class7	18	309.83	-13.27	3.55	0	0

Frozen land duration class	Total number of pixels (N)	Mean FL89	Mean Temp89	SD Temp89	Mean GPP89	SD GPP89
class1	3416	23.45	11.17	3.43	26.51	17.86
class2	2662	74.5	7.02	3.64	23.56	17.21
class3	3910	125.55	2.78	3.85	23.22	14.42
class4	3977	174.51	-0.8	3.71	27.3	11.09
class5	4458	220.94	-8.75	4.32	15.88	7.87
class6	1244	265.59	-12.29	2.86	5.53	4.49
class7	155	316.34	-14.72	2.64	0.38	1.58

## CONCLUSIONS

Results from the monthly average area of frozen land (sq km) and the chi-square values shows that the amount of land that was frozen and thawed during the 1997-98 El Niño and the 1988-89 La Niña events is not similar. Thus, the impact of both events on the land surface process is different. There was a decrease in total average frozen land of approximately 0.7 million sq km in North America and approximately 0.33 million sq km in Northern Eurasia from 1988-89 La Niña to 1997-98 El Niño. This can be explained as the number of El Niño events that occurred in the decade of 1990 (Trenberth, 1997) are more. There is a direct relationship between the El Niño years and the reduced snow cover extent (Kimball, et al. 2001). Hence, this decrease in the frozen land area during the El Niño event can be supported as the decrease in amount of snow extent during El Niño years.

The difference in the frozen land area (sq km) between preceding months indicates the change in the transition period between freezing and thawing. North America during the 1997-98 El Niño event froze a month earlier (August) and thawed a month earlier (February) than the 1988-89 La Niña event. However, not any difference in transition between freezing and thawing of land surface is seen between the two events for Northern Eurasia.

The correlation between the average duration of frozen land and average air temperature as well as average duration of frozen land and average GPP is negative. However, the correlation between the average air temperature and average GPP is positive. The relation between the average duration of frozen land and average air temperature is concentrated and the relation between the duration of frozen land and average GPP is scattered or dispersed. Nevertheless, a strong linear relationship is found for North America but not for Northern Eurasia (except for average duration of frozen land Vs air temperature).



The variation of air temperature as well as GPP with in each class of frozen land duration is more or less same for North America and Northern Eurasia respectively. It is observed from high-low bars that for almost all classes of frozen land duration, the variation of air temperature is similar for both regions between the two events. The average air temperature decreased along the frozen land duration. While variation of GPP with in a class and average GPP was higher for the first four classes of frozen land duration and kept fluctuating for these four classes but later the variation and average GPP decreased for remaining classes.

Hence, unlike North America, Northern Eurasia had lesser difference of average frozen land (sq km) between the 1988-89 La Niña and the 1997-98 El Niño events, had no change in the transition between freezing and thawing between these events and had no a clear association among the attributes. This can be due to the other climatic variations such as North Atlantic Oscillation (NAO) other than MEI, affecting the land surface processes of Northern Eurasia (Franzke, et al. 2002).

## **FUTURE RESEARCH RECOMMENDATIONS**

Although this study remains as a case study due to insufficient data, I strongly recommend that this study should be continued. It is found that the frequency of the El Niño and La Niña events is increasing (Timmermann, et al. 1999) since the 1970s and the importance of global climatic conditions on vegetation is well documented (Myneni, et al. 1997). The percent of decrease in frozen land area from 1988-89 to 1997-98 is found to be 13%, on average, in North America and 10% in Northern Eurasia.

The increase or decrease in the amount of frozen land area effects the energy absorbed or released by the land surface. The variations in the surface energy influence the heat stored, released and transferred by the land thus influencing the climate such as the air temperature and precipitation. The computed percent of increase or decrease in frozen land area between the events with 1988-89 as the base year (Figure 6) shows that there is a huge difference in frozen land during summers (between 25-50%) and not much during winters (between 5-12%). The decrease in the amount of frozen land leads to increases in terrestrial temperatures. This increase in air temperature and decrease in frozen land can be related to El Niño and La Niña events that are leading to global warming.

As well as the air temperature, land surface processes affect all of us; the relationship between the climatic and land surface processes should be further explored. The data sets used in this study (air temperature, freeze/thaw and GPP) should be acquired for all El Niño and La Niña events that have occurred from at least 1970s and the general behavior pattern of these attributes should be investigated. I also recommend studying the degree of spatial variation due to ENSO at different climatic zones (boreal, temperate and sub tropical) as the amount of decrease in frozen land area is greater in North America (Figure 6).

## REFERENCES

- Armstrong, R. L. and M. J. Brodzik. 1995. An Earth-Gridded SSM/I Data Set for Cryospheric Studies and Global Change Monitoring, *Advanced Space Research* 16(10): 155-163.
- Armstrong, R.L. and M. J. Brodzik. 1999. A Twenty Year Record of Global Snow Cover Fluctuations Derived from Passive Microwave Remote Sensing Data, in *Proceedings of the Fifth Conference on Polar Meteorology and Oceanography*, 10-15 January 1999, Dallas, Texas, American Meteorological Society, pp. 113-117.
- Diaz, H. F. and V. Markgraf. 2000. *El Niño and the Southern Oscillation Multiscale Variability and Global and regional Impacts*, Cambridge University Press: 496 pp.
- Franzke, C. and S. Feldstein. 2002. Science Daily News Release: North Atlantic Oscillation part of the Global Picture. Research Presented at the fall meeting of the American Geophysical Union by Pennsylvania State University.  
<http://www.sciencedaily.com/releases/2002/12/021212080940.htm>.
- Goodison, B. E. 1989. Determination of areal snow water equivalent on the Canadian prairies using passive microwave satellite data, IGARSS'89, 12<sup>th</sup> Canadian Symposium on Remote Sensing, Quantitative Remote Sensing: An economic tool for the nineties, Vancouver, Canada, July 10-14, 1989, 3: 1243-1246.
- Harrison, J. and M. Halpert. 2002. National Weather Service, Climate Prediction Center. The Southern Oscillation Index.  
[http://www.cpc.ncep.noaa.gov/products/analysis\\_monitoring/ensocycle/soi.html](http://www.cpc.ncep.noaa.gov/products/analysis_monitoring/ensocycle/soi.html)
- Hershfield, D. M. 1974. The frequency of freeze/thaw cycles. *Journal of Applied Meteorology* 13: 348-354.
- Judge, J., J. F. Galantowicz, A. W. England and P. Dahl. 1996. Freeze/thaw classification for Prairie soils using SSM/I radiobrightness Remote Sensing for a Sustainable Future, IGARSS'96, Burnham Yates Conference Center, Lincoln, Nebraska, USA, 27-31 May 1996, *IEEE* 4(2): 270-272.
- Kimball, J. S., K.C. McDonald, A.R. Keyser, S. Frolking and S.W. Running, 2001. Application of the NASA Scatterometer (NSCAT) for Determining the Daily Frozen and Non-frozen Landscape of Alaska, *Remote Sensing Environment* 75: 113-126.
- Langenberg, H., Senior Editor. 2002. Climate and Water, *Nature* 419(6903): 187.
- Legates, D. R. and C. J. Willmott. 1990a. Mean Seasonal and Spatial Variability in Global Surface Air Temperature, *Theoretical and Applied Climatology* 41: 11-21.

- Myneni, R. B., R. R. Nemani and S. W. Running, 1997a. Estimation of Global Leaf Index and Absorbed Par using Radiative Transfer Models, *IEEE Transactions on Geoscience and Remote Sensing* 35(6): 1380-1393.
- Myneni, R. B., C. D. Keeling, C. J. Tucker, G. Asrar, and R. R. Nemani, 1997b. Increased Plant Growth In: The Northern High Latitudes from 1981 to 1991, *Nature* 386: 698-702.
- Neelin, J. D. and M. Latif. 1998. El Niño Dynamics, *Physics Today*: 32-36.
- Nemani, R. R., C. D. Keeling, H. Hashimoto, W. M. Jolly, S. C. Piper, C. J. Tucker, R. B. Myneni, S. W. Running. 2003. Climate-Driven Increases in Global terrestrial Net Primary Production from 1982 to 1999. *Science* 300: 1560-1563.
- Pierrehumbert, R. 2000. Climate change and the tropical Pacific: The sleeping dragon wakes. *Proc. National Acad. Science* 97(4): 1355-1358.
- Running, S. W., J. S. Kimball, A. R. Keyser, J. B. Way, K. C. McDonald, S. Frolking and R. Zimmerman, 1999a. Recent Advances in Satellite Radar Remote Sensing Proposed for Monitoring Freeze/Thaw transitions in Boreal Regions, *Eos, Transactions, American Geophysical Union* 80(19): 213,220-221.
- Running, S. W., R. R. Nemani, J. M. Glassy and P. E. Thornton, 1999b. MODIS daily photosynthesis (PSN) and annual net primary production (NPP) product (MOD17), Algorithm Theoretical Basis Document Version 3.0.
- Slingo, J. 1998. The 1997/98 El Niño, *Weather* 53(9): 274 – 281.
- Trenberth, K. E. 1997. The Definition of El Niño, *Bulletin of the American Meteorological Society* 78(12): 2771 – 2776.
- Varani, A. NSIDC. 2000. Frozen Soils and the Climate System, *Earth System Monitor* 11(1): 1-2.
- Visser, K., R. Thunell and L. Scott. 2003. Magnitude and timing of temperature change in the Indo-Pacific warm pool during deglaciation. *Nature* 421: 152-155.
- Webster, P. J. and T. N. Palmer. 1997. The past and future of El Niño, *Nature* 390: 562 - 564.
- Wolter, K. and M. S. Timlin. 1998. Measuring the strength of ENSO events: How does 1997-98 rank?, *Weather* 53(9): 315 – 324.
- Wolter, K. and M. S. Timlin. 1993. Monitoring ENSO in COADS with a seasonally adjusted principal component index. In: *Proceedings of the 17<sup>th</sup> Climate Diagnostics Workshop*, Norman, Oklahoma, pp. 52-57.

Wolter, K. 2002. Multivariate ENSO Index (MEI), NOAA-CIRES Climate Diagnostics Center. <http://www.cdc.noaa.gov/~kew/MEI/mei.html>

Zhang, T., T. E. Osterkamp and K. Stamnes. 1996. Influence of the depth hoar layer of the seasonal snow cover on the ground thermal regime, *Water Resources Research* 32(7): 2075-2086.

Zhang, T., R. Armstrong and J. Smith. 1999. Detecting Seasonally Frozen Soils Over Snow-free Land Surface using Satellite Passive Microwave Remote Sensing Data, in the Proceedings of the Fifth Conference on Polar Meteorology and Oceanography, 10-15 January 1999, Dallas, Texas, pp. 355-357.

## GLOSSARY

**Albedo:** The fraction of the incident electromagnetic radiation that is reflected by the surface.

**Brightness Temperature:** Brightness temperature or apparent temperature is the emissivity or radiation between the objects at same temperature measured by the microwave radiometer in the microwave portion of the spectrum.

**El Niño Southern Oscillation Index (ENSO):** ENSO phenomenon is considered as a part of global climate system and results from large-scale interactions between the oceans and the atmosphere that occur chiefly across its core region in the tropical-subtropical Pacific to Indian Ocean basins.

**Equal Area Scalable Earth (EASE) Grid:** The EASE Grid format was developed by the NSIDC for the MASA/NOAA Pathfinder program level 3 products which include both SSM/I and SMMR data.

**FPAR:** It is the fraction of absorbed Photosynthetically Active Radiation (PAR).

**PAR:** Photosynthetically Active Radiation is the radiation that can be used for the process of photosynthesis.

**Gross Primary Production (GPP):** It is the total amount of carbon produced by plants per unit time and area in the process of photosynthesis. Usually measured in Kg C/m<sup>2</sup>/day.

**Normalized Difference of Vegetation Index (NDVI):** It is the ratio of difference between the reflectance of near infrared region and the visible region to the total reflectance of near infrared and visible region observed by the Advanced Very High Resolution radiometer onboard the National Oceanic Atmospheric Administration Satellite.

**APPENDIX**

**FIGURE 1**

**EQUAL AREA SCALABLE EARTH (EASE) GRID PROJECTION.  
GRID SIZE – 25 KM X 25 KM.  
THE DIFFERENCE BETWEEN THE 1997-98 EL NIÑO AND THE 1988-89 LA  
NIÑA EVENTS.**

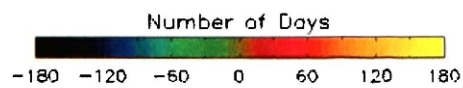
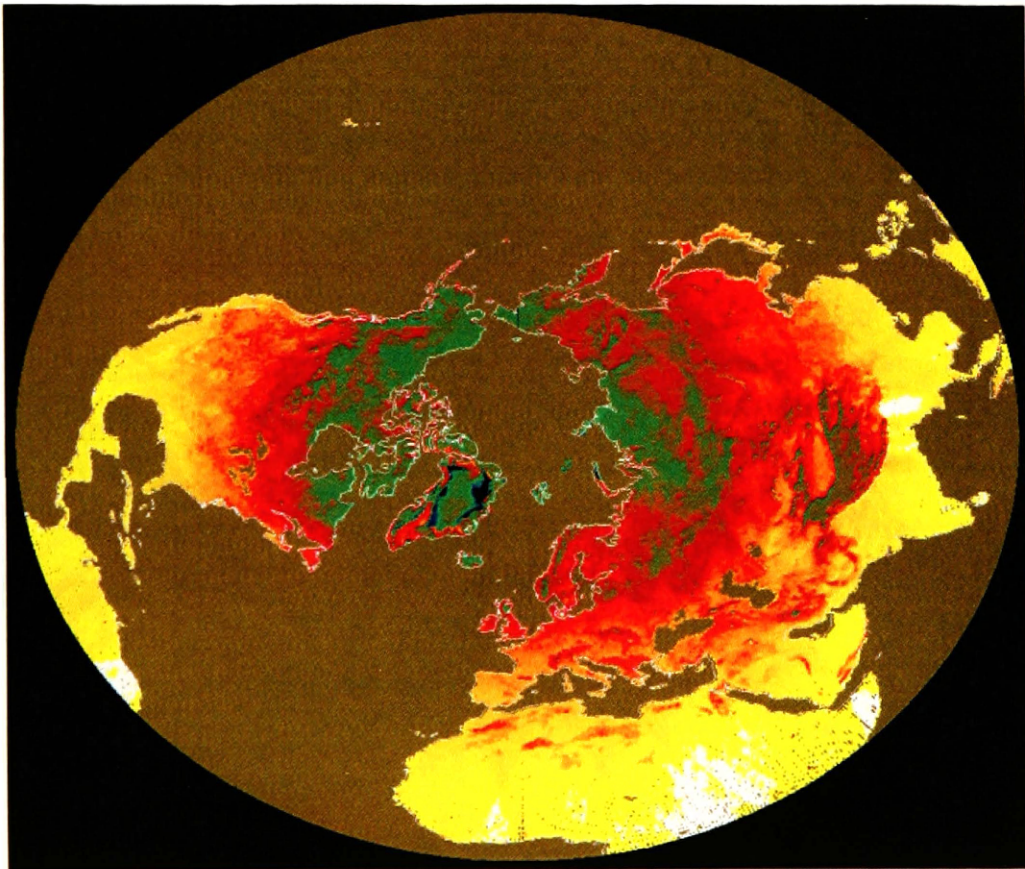




**FIGURE 2**

**GEOGRAPHIC PROJECTION.  
EQUAL LATITUDE AND LONGITUDE OF SIZE 0.5°.  
DIFFERENCE BETWEEN THE 1997-98 EL NIÑO AND THE 1988-89 LA NIÑA  
EVENTS.**

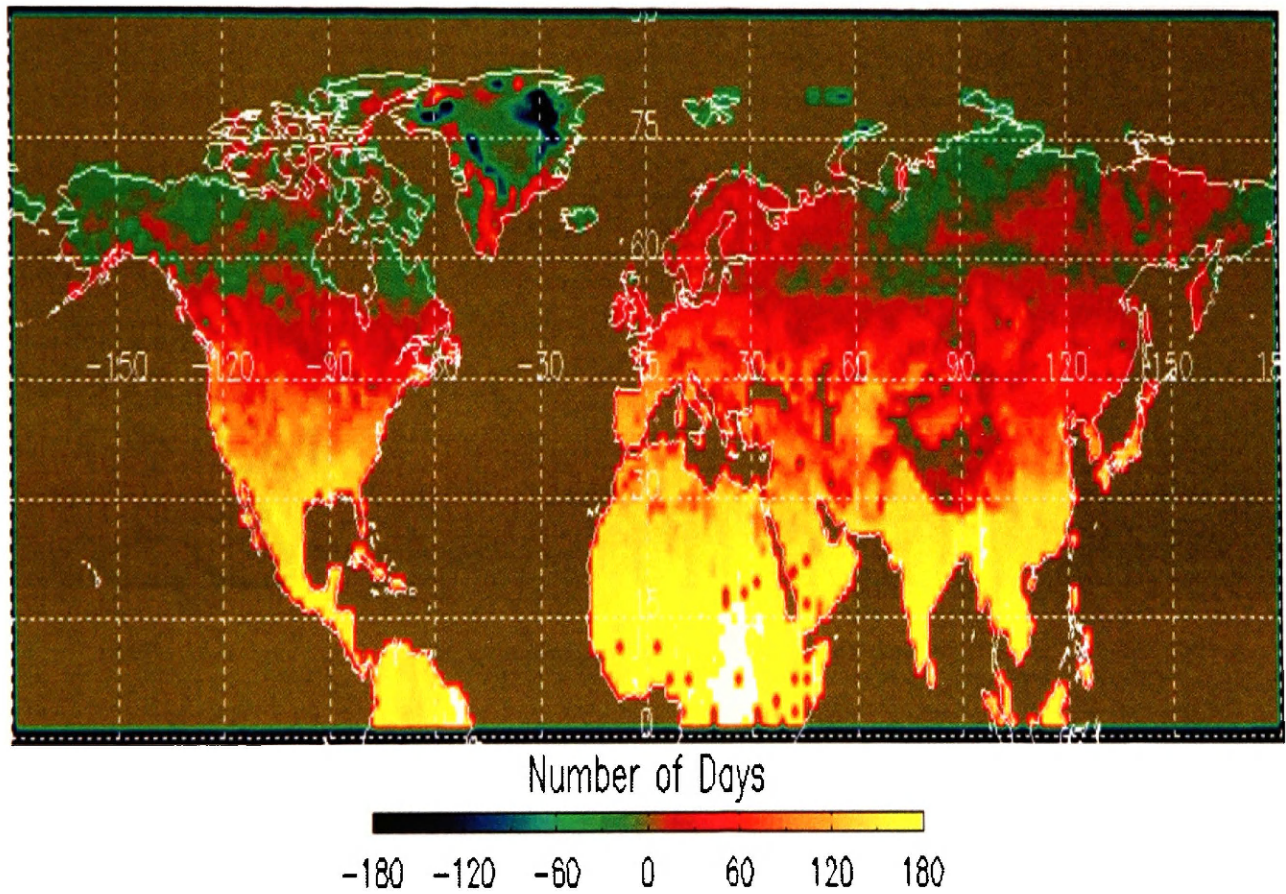
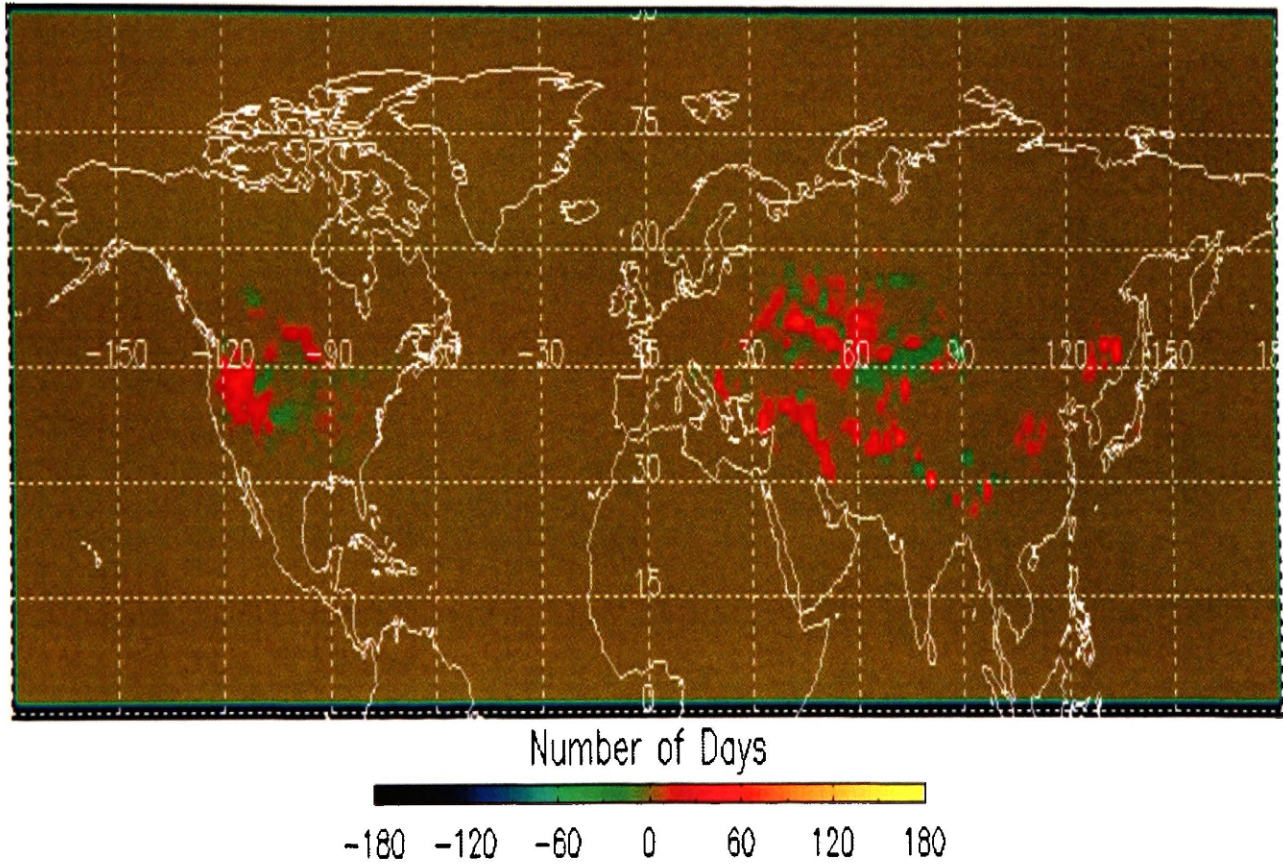




**FIGURE 3**

**DIFFERENCE IN NON-FROZEN BARE GROUND  
BETWEEN THE 1997-98 EL NIÑO AND THE 1888-89 LA NIÑA EVENTS.**



**PROGRAM 1**  
**PROGRAM TO CONVERT THE EASE-GRID FREEZE/THAW DATA TO**  
**GEOGRAPHIC PROJECTION.**

```

pro EASE_Geog
; PURPOSE:
; converts azimuthal equal-area or equal-area cylindrical grid coordinates
; to geographic coordinates.
; EASE Grid Map is of Northern Hemisphere (with latitude ranging from
; 0-90 degree and longitude ranging from -180 to +180 degrees)
EASE = ftarr(721,721)
cols = 721
rows = 721
RE_km = 6371.228
CELL_km = 25.067525
latt = (90-0)/0.25 ;0.25 is the resolution in degrees
long = (180-(-180))/0.25
output = ftarr(long,latt)
Geog = ftarr(long,latt)
dir = '/u1/divya/pro'
for cat = 1,8 do begin
    file_name = 'diff' + strtrim(cat,2)
    file = filepath(root_dir = dir, file_name)
    close, 1
    openr, 1, file, ERROR = err
    if (err eq 0) then begin
        readu, 1, EASE
    endif else print, 'file not found', file
    close, 1
endfor
for i = 0,720 do begin
    for j = 0,720 do begin
        scale = 1 ;Assume grid projection to be 25 km
        Rg = scale * RE_km/CELL_km
        r0 = (cols-1)/2. * scale ;center of the grid
        s0 = (rows-1)/2. * scale ;center of the grid
        x = i - r0
        y = j - s0
        rho = sqrt(x*x + y*y) ;radial distance from center
        if rho eq 0. then begin
            lat = 90.0
            lon = 0.0
        endif else begin
            sinphil = sin(!PI/2.)
            cosphil = 0
            if y eq 0. then begin

```

```

        if i le r0 then lam = -!PI/2.
        if i gt r0 then lam = !PI/2.
    endif else begin
        lam = atan(x,-y)
    endelse
gamma = rho/(2 * Rg) ;gamma is the rho value for diameter = 1
if (abs(gamma) gt 1.0) then GOTO, Invalid
    c = 2 * asin(gamma)
    beta = cos(c) * sinphil
endelse
if (abs(beta) gt 1.) then GOTO, Invalid
    phi = asin(beta) ; phi is rho value for radius equal = 1
    lat = phi * 180/!PI ;converting radians to degrees
    lon = lam * 180/!PI ;converting radians to degrees
if (lat lt 0.0) then GOTO, Invalid
m = long * ((lon+180)/360.)
n = latt * ((90-lat)/90.0)
m = fix(m) ; floating to integer
if (m eq 1440) then m = 0
n = fix(n) ; floating to integer
output[m,n] = EASE[i,j]
Invalid:
    endfor
endfor
output = congrid(output,720,180) ;resizes the grid from 1440*360 to 720*180
output = reverse(output, 1)
openw, 1, output
writeu, 1, Geog
END

```

## PROGRAM 2

THE MISSING AND OCEAN/LAKE DATA ARE KEPT IN ONE CATEGORY.  
 NORTH AMERICA AND NORTHERN EURASIA ARE EXTRACTED FROM  
 NORTHERN HEMISPHERE

```

dummy = fltarr(313,180,704)
;North America = (313,180,704) and Eurasia = (390,180,704)
dummy1= fltarr(313,161,704)
;North America and = (313,161,704) and Northern Eurasia = (390,110,704)
for i=0,389 do begin
for j=0,109 do begin
    for k=0,351 do begin
        if (dummy[i,j,k] eq 7) OR (dummy[i,j,(k+352)] eq 7) or (dummy[i,j,k] eq
8) OR (dummy[i,j,(k+352)] eq 8) then begin
            dummy1[i,j,k] = 5
        end
    end
end
end

```

```

        dummy1[i,j,k+352] = 5
    endif else begin
        dummy1[i,j,k] = dummy[i,j,k]
        dummy1[i,j,k+352] = dummy[i,j,k+352]
    endelse
endfor
endfor
endfor
close, 9
openw, 9, 'ntsg/divya/final/northern_eurasia/category98.dat'
writeu, 9, dummy1
close, 9

```

### PROGRAM 3

MONTHLY AVERAGE NUMBER OF PIXELS AND AVERAGE AREA (sq km) OF EACH CATEGORY

```

dummy = ftarr(313,161,704)
dummy1 = ftarr(313,161,31)
day_cat = ftarr(313,161,5)
close, 9
openr, 9, 'ntsg/divya/final/america/category98.dat'
readu, 9, dummy
close, 9

```

**;k values are changed when calculated for month and year.**

```

for i = 0,312 do begin
    for j = 0,160 do begin
        for k=0,30 do begin
;for yearly calculation 1988-89 k=352,703 and 1997-98 k=0,351
            dummy1[i,j,*]=dummy[i,j,k] ;whereas for 1988-89 it is dummy[i,j,(k-351)]
        endfor
    endfor
endfor

```

```

for i = 0,312 do begin
    for j = 0,160 do begin
index1 = dummy1[i,j,*] eq 1
n1 = total(index1)
day_cat[i,j,0] = n1
index2 = dummy1[i,j,*] eq 2
n2 = total(index2)
day_cat[i,j,1] = n2
index3 = dummy1[i,j,*] eq 3
n3 = total(index3)
day_cat[i,j,2] = n3
index4 = dummy1[i,j,*] eq 4

```

```

n4 = total(index4)
day_cat[i,j,3] = n4
index5 = dummy1[i,j,*] eq 5
n5 = total(index5)
day_cat[i,j,4] = n5
    endfor
endfor
; count_pixel values are used in chi-square test.
count_pixel = lonarr(5)
for i = 0,4 do begin
count_pixel[i] = total(day_cat[*,* ,i])/31
endfor

temp=dblarr(720,360)
area=dblarr(313,161)
openr, 1, '/ntsg/divya/eurasia/halfdeg.area'
readu,1,temp
close,1
for i=15,327 do begin
    for j=0,160 do begin
        area[i-15,j]=temp[i,j]
    endfor
endfor
;area of each category in freeze/thaw data.
month_area = dblarr(5)
for i = 0,4 do begin
    month_area[i]=0.0
    for j=0,312 do begin
        for k=0,160 do begin
            month_area[i]=month_area[i]+(day_cat[j,k,i]*area[j,k])/31.00
        endfor
    endfor
endfor
close, 9
openw, 9, '/ntsg/divya/final/america/numofdays_jan98.dat'
writeu, 9, day_cat
close, 9
close, 9
openw, 9, '/ntsg/divya/final/america/pixel_count_jan98.txt'
printf, 9, count_pixel
close, 9
close, 9
openw, 9, '/ntsg/divya/final/america/area_jan98.txt'
printf, 9, month_area
close, 9

```

end

**PROGRAM 4**  
THE MAXIMUM NUMBER OF DAYS THAT A PIXEL BELONGS IN ONE  
CATEGORY FOR A YEAR.

```
pro pixel
dummy = fltarr(390,110,704)
;north America=(313,161) northern Eurasia=(390.110)
output = intarr(390,110)
count = lonarr(4)
sum = lonarr(4)
sum[*] = 0
for i = 0,389 do begin
    for j = 0,109 do begin
        count[*] = 0L
        for k = 352,703 do begin
;k=0,351 or 352,703. one year is considered at a time.
            if (dummy[i,j,k] eq 1) then begin
                count[0] = count[0]+1
            endif
            if (dummy[i,j,k] eq 2) then begin
                count[1] = count[1]+1
            endif
            if (dummy[i,j,k] eq 3) then begin
                count[2] = count[2]+1
            endif
            if (dummy[i,j,k] eq 4) then begin
                count[3] = count[3]+1
            endif
        endfor
        if (count[0] eq 0 AND count[1] eq 0 AND count[2] eq 0 AND count[3] eq 0) then
begin
            output[i,j] = 5
        endif
        if (count[0] gt count[1]) AND (count[0] gt count[2]) AND (count[0] gt count[3])
then begin
            output[i,j] = 1
        endif
        if (count[1] gt count[0]) AND (count[1] gt count[2]) AND (count[1] gt count[3])
then begin
            output[i,j] = 2
        endif
        if (count[2] gt count[0]) AND (count[2] gt count[1]) AND (count[2] gt count[3])
then begin
```

```

        output[i,j] = 3
    endif
    if (count[3] gt count[0]) AND (count[3] gt count[1]) AND (count[3] gt count[2])
then begin
        output[i,j] = 4
    endif
    sum[*] = sum[*]+count[*]
endfor
endifor
close, 9
openw, 9, '/ntsg/divya/final/northern-eurasia_pixel_map98.dat'
writeu, 9, output
close, 9

end

```

### PROGRAM 5

OVERLAPPING THE FREEZE/THAW DATA WITH TEMPERATURE DATA TO ELIMINATE THOSE PIXELS IN TEMPERATURE DATA THAT REPRESENT AS MISSING PIXELS IN FREEZE/THAW DATA. THE AVERAGE MONTHLY AIR TEMPERATURE IS ALSO OBTAINED SIMULTANEOUSLY

```

pro temp_clip
;output file has temp values for those pixels for which NGBF+FBG+NFSC+FSC
;values are available
table = fltarr(720,360,12)
dummy = fltarr(313,161,12)
close, 9
openr, 9, '/ntsg/divya/north_america/tave.1997.mon'
readu, 9, table
close, 9
for i = 6,11 do begin
dummy[*,*(i-6)] = table[15:327,0:160,i]
;northamerica-15:327, 0:160, northernEurasia-330-719,0:109
endfor
close, 9
openr, 9, '/ntsg/divya/north_america/tave.1998.mon'
readu, 9, table
close, 9
for i = 0,5 do begin
dummy[*,*(i+6)] = table[15:327,0:160,i]
endfor
dummy1 = intarr(313,161)
close, 9
openr, 9, '/ntsg/divya/final/america_pixel_map98.dat'
readu, 9, dummy1

```

```

close, 9
temp1 = dblarr(720,360)
area = dblarr(313,161)
openr, 1, '/ntsg/divya/eurasia/halfdeg.area'
readu, 1, temp1
close, 1
for i = 15,326 do begin      ;northAmerica-15,326, northernEurasia-330,719
    for j = 0,160 do begin
        area[i-15,j] = temp1[i,j]
    endfor
endfor
temp2 = fltarr(313,161,12)
sum = fltarr(12)
sum[*] = 0.0

    for i = 0,312 do begin
        for j = 0,160 do begin
            for k = 0,11 do begin
                if (dummy1[i,j] ne 5) then begin
                    temp2[i,j,k] = dummy[i,j,k]*area[i,j]
                    sum[k]=sum[k]+area[i,j]
                endif
            endfor
        endfor
    endfor
endfor
avet = fltarr(12)
for i = 0,11 do begin
    avet[i] = total(temp2[*],*,i)/sum[i]
endfor
close, 9
openw, 9, '/ntsg/divya/final/america-temp98.txt'
printf, 9, avet
close, 9
end

```

### PROGRAM 6

OVERLAPPING THE FREEZE/THAW DATA WITH GPP DATA TO ELIMINATE THOSE PIXELS IN GPP DATA THAT REPRESENT AS MISSING PIXELS IN FREEZE/THAW DATA.THE AVERAGE MONTHLY GPP IS ALSO OBTAINED SIMULTANEOUSLY

```

pro gpp_clip
;output file has temp values for those pixels for which NGBF+FBG+NFSC+FSC
;values are available
;gpp input data is in kg C/m2/day
A = fltarr(12,8,720,360)

```



```

B = fltarr(12, 390,110)
close, 1
openr, 1, '/ntsg/divya/gpp/1988_metsum_month_v1.bsq'
readu, 1, A
close, 1
for i = 6,11 do begin
B[(i-6),*,*] = A[i,7,330:719,0:109]
;northAmerica-14:326,0:160, northernEurasia-330:719,0:109
endfor
openr, 1, '/ntsg/divya/gpp/1989_metsum_month_v1.bsq'
readu, 1, A
close, 1

for i = 0,5 do begin
B[(i+6), *, *] = A[i,7,330:719,0:109]
endfor
table = intarr(390,110)
close, 1
openr, 1, '/ntsg/divya/final/northern_eurasia_pixel_map89.dat'
readu, 1, table
close, 1
temp = dblarr(720,360)
area = dblarr(390,110)
openr, 1, '/ntsg/divya/eurasia/halfdeg.area'
readu, 1, temp
close, 1
for i = 330,719 do begin      ;northAmerica-15,326, northernEurasia-330,719
    for j = 0,109 do begin
        area[i-330,j] = temp[i,j]
    endfor
endfor

dummy = fltarr(12,390,110)
sum = fltarr(12)
sum[*] = 0.0
    for i = 0,389 do begin
        for j = 0,109 do begin
            for k = 0,11 do begin
                if (table[i,j] ne 5) AND (B[k,i,j] gt 0) then begin
                    dummy[k,i,j] = B[k,i,j]*area[i,j]
                    sum[k]=sum[k]+area[i,j]
                endif
            endfor
        endfor
    endfor
!order = 1

```

```

window, 0
tvsc1, dummy[0,*,*]
gpp_month = ftarr(12)
for i = 0,11 do begin
gpp_month[i] = total(dummy[i,*,*])/sum[i]
endfor
close, 1
openw, 1, '/ntsg/divya/final/northern_eurasia_gpp_month89.txt'
printf, 1, transpose(gpp_month)
close, 1
openw, 1, '/ntsg/divya/final/northern_eurasia_gpp-month89.dat'
writeu, 1, dummy
close, 1
end

```

### PROGRAM 7

CORRELATION AMONG AVERAGE DURATION OF FROZEN LAND, AVERAGE AIR TEMPERATURE AND AVERAGE GPP.

```

pro corre
dummy = ftarr(390,110,5) ;NA = (313,161)
y = ftarr(390,110) ;air temperature
z = ftarr(390,110) ;GPP

z = z*1000 ; converting GPP from Kg C/m2/year to g C/m2/year
x = ftarr(390,110) ;frozen=frozen bare ground-1 and frozen snow cover-3
x[*,*] = dummy[*,*,1]+dummy[*,*,3]
!P.Font = 1
DEVICE, SET_FONT = 'Helvetica'
ind=where(y[*,*] ne 0.0 and y[*,*] ne -999.0 and z[*,*] ne -999.0)
tvlct, 255,255,255,0
tvlct, 0,0,0,1
!P.Background = 0
plot, y[ind[*]], z[ind[*]], psym=1,symsize=0.5, color = 1
result = correlate(y[ind[*]],z[ind[*]]) ; done for two variables at a time
xyouts, 0.745,0.87, 'r = ', color=1,charsize=2.0,charthick=1.5,/normal
xyouts, 0.75,0.87,result, color=1, charsize=2.0,charthick=1.5,/normal
print, result
end

```

### PROGRAM 8

OBTAIN AIR TEMPERATURE AND GPP DATA FOR THE FROZEN LAND DURATION CLASSES

```

pro class_division
dummy1 = ftarr(313,161,5) ;NE=(390,110)
dummy2 = ftarr(313,161) ;air temperature
dummy3 = ftarr(313,161) ;GPP

x=ftarr(313,161) ;frozen land
x[*,*] = dummy1[**,1] + dummy1[**,3]
;frozen land=frozen bare ground- 1 and frozen snow cover-3.
dummy3[*,*] = dummy3[*,*]*1000 ;Converting Kg C/m2/year to g C/m2/year
;the bold numbers are the beginning and ending of class 7 of frozen land duration –
refer Table 3. For each class the numbers in bold change accordingly.
for i = 0, 312 do begin
    for j = 0, 160 do begin
        if (300 le x[i,j]) and (x[i,j] lt 350) and (dummy2[i,j] ne 0.0) and
            (dummy2[i,j] ne -999.0) and (dummy3[i,j] ne -999.0) then begin
            close, 1
            openw, 1, '/ntsg/divya/final/classes/northern_eurasia_temp_class7.txt'
            printf, 1, transpose(dummy2[i,j])
            close, 1
            close, 1
            openw, 1, '/ntsg/divya/final/classes/northern_eurasia_gpp_class7.txt'
            printf, 1, transpose(dummy3[i,j])
            close, 1
            endif
        endifor
    endfor
endfor
end

```

**Monthly Average Frozen Land Area (sq km) of North America and Northern Eurasia during the 1988-89 La Niña and 1997-98 El Niño events**

**Non-Frozen Land (NFBG) and Frozen Land (FBG+FSC)**

North America Area(Sq km)	Non-Frozen Land	Frozen Land98	Non-Frozen Land	Frozen Land89
July	17683689	1755320.95	16376198	3062731.1
Aug	17310694	1949168.5	16789307	2470362.87
Sep	16191700	2709108.07	15978405	2922722.5
Oct	14266348	5240991.5	14664068	4843994.3
Nov	9684587.3	10087913.4	10471946	9312807.7
Dec	6999158	13039825.1	6707234.4	13360100.6
Jan	5111997.3	14269785.2	4826293.5	14441374.7
Feb	5906170.2	13958449.9	4640800.7	14940071.2
Mar	5977576.3	12730819.1	5475997.4	13189261.5
Apr	9505355.5	10612157.4	8101685.3	12014019.6
May	14017342	5568257.9	12065470	7524693
Jun	17470626	2154134.5	15254515	4374504.6
	140125243.6	94075931.52	131351920.3	102456643.7

Northern Eurasia Area(Sq. km)	Non-Frozen Land	Frozen Land98	Non-Frozen Land	Frozen Land89
July	27571815	987171.35	27191056	1356146.74
Aug	28958185	512165.45	28737041	722338.03
Sep	27950263	1303036.46	27573178	1669124.07
Oct	22100232	6987171	22887532	6190030.1
Nov	12534111	16353872.2	11403850	17472885
Dec	6847550.4	22879909.7	6328406.5	23319207.1
Jan	4430281.1	23502649.3	4148730	23754546.3
Feb	5018891.4	23302856	4654592.3	23548225.1
Mar	5923318.8	20974344.3	6763079	20260499.7
Apr	12837131	16730622.9	12037675	17385623.7
May	20784851	8901462.9	20327842	9344948.9
Jun	27155354	2134143.2	25770263	3501447.3

**CHI SQUARE TEST**

H<sub>0</sub> : The distribution at a point of time is homogenous for the two data sets.

H<sub>a</sub> : Reject H<sub>0</sub>

Test Statistic:

$$X^2_c = \sum_{i=1}^r \sum_{j=1}^c (O_{ij} - E_{ij})^2 / E_{ij}$$

where O<sub>ij</sub> = observed cell count or frequency

E<sub>ij</sub> = expected cell count or frequency

$$= (\text{row total}_i)(\text{column total}_j) / \text{grand total}$$

r = number of rows

c = number of columns

Rejection Rule : Reject H<sub>0</sub> if  $X^2_c > X^2_{(r-1)(c-1), \alpha}$

## Chi-Square Values for frozen and non-frozen pixels of North America

Average Nui	July	Aug	Sep	Oct	Nov	Dec	Jan	Feb	Mar	Apr	May	Jun	
NFBG98	10932	10575	9481	7946	4938	3483	2560	2867	2944	4930	7928	10895	953748
FBG98	1426	1728	2594	3846	5035	4190	2786	2401	2066	1945	1624	1355	371952
FSC98	720	682	667	1358	3301	5747	7765	8066	7516	6570	3632	1002	564312
NFBG89	9688	9943	9340	8170	5303	3269	2288	2200	2584	3969	6428	8839	864252
FBG89	2071	2010	2691	3876	5246	4441	2773	2689	2289	2167	2067	1938	411096
FSC89	1317	1032	711	1104	2730	5722	8000	8322	7631	7308	4691	2477	612540

### Chi-Square Test

#### Observed Values

Frozen Land July	Aug	Sep	Oct	Nov	Dec	Jan	Feb	Mar	Apr	May	Jun	Row Total	
1997-1998	2146	2410	3261	5204	8336	9937	10551	10467	9582	8515	5256	2357	78022
1988-1989	3388	3042	3402	4980	7976	10163	10773	11011	9920	9475	6758	4415	85303
Column Total	5534	5452	6663	10184	16312	20100	21324	21478	19502	17990	12014	6772	
													Grand Total
													163325

#### Expected Values

Frozen Land July	Aug	Sep	Oct	Nov	Dec	Jan	Feb	Mar	Apr	May	Jun	
1997-1998	2643.648	2604.48	3182.98	4865	7792.407	9602	10187	10260	9316.3021	8594	5739.21	3235.1
1988-1989	2890.352	2847.52	3480.02	5319	8519.593	10498	11137	11218	10185.698	9396	6274.79	3536.9
1997-1998	93.67858	14.5214	1.91228	23.62206	37.92069	11.69	13.029	4.1658	7.5776163	0.72629	40.6835	238.32
1988-1989	85.68269	13.282	1.74906	21.60581	34.68398	10.692	11.917	3.8103	6.9308322	0.66429	37.2109	217.98

934.0529 with df=11

#### Observed Values

Non-Frozen July	Aug	Sep	Oct	Nov	Dec	Jan	Feb	Mar	Apr	May	Jun	Row Total	
1997-1998	10932	10575	9481	7946	4938	3483	2560	2867	2944	4930	7928	10895	79479
1988-1989	9688	9943	9340	8170	5303	3269	2288	2200	2584	3969	6428	8839	72021
Column Total	20620	20518	18821	16116	10241	6752	4848	5067	5528	8899	14356	19734	
													Grand Total
													151500

#### Expected Values

Non-Frozen July	Aug	Sep	Oct	Nov	Dec	Jan	Feb	Mar	Apr	May	Jun	
1997-1998	10817.54	10764	9873.76	8454.677	5372.571	3542.2	2543.3	2658.2	2900.0654	4668.54	7531.36	10353
1988-1989	9802.462	9753.97	8947.24	7661.323	4868.429	3209.8	2304.7	2408.8	2627.9346	4230.46	6824.64	9381.3
1997-1998	1.211143	3.31951	15.6231	30.60463	35.15106	0.9892	0.1093	16.398	0.6655873	14.6431	20.8895	28.404
1988-1989	1.336561	3.66325	17.2409	33.77384	38.79107	1.0916	0.1206	18.096	0.734511	16.1595	23.0526	31.345

353.4136 with df = 11

Note: NFBG = Non-Frozen Bare Ground  
 FBG = Frozen Bare Ground  
 NFBG = Non-Frozen Snow Cover  
 FSC = Frozen Snow Cover

## Chi-Square Values for frozen and non-frozen pixels of Northern Eurasia

Average nur July	Aug	Sep	Oct	Nov	Dec	Jan	Feb	Mar	Apr	May	June	
NFBG98	16473	17417	16802	12614	6523	3394	2191	2424	2807	6257	11102	15852
FBG98	360	229	636	2658	4043	3690	2314	2066	1963	1360	887	528
FSC98	422	129	205	2292	6898	10827	12483	12782	11587	10210	5909	1318
NFBG89	16151	17247	16425	13189	5861	3081	2064	2309	3309	5953	10961	14809
FBG89	434	359	1011	2986	4746	3574	2157	2151	1901	1916	1199	876
FSC89	660	158	198	1380	6847	11213	12748	12765	11198	9872	5727	2000

### Observed Values

Frozen Land July	Aug	Sep	Oct	Nov	Dec	Jan	Feb	Mar	Apr	May	June	Row Total		
1997-1998	782	358	841	4950	10941	14517	14797	14848	13550	11570	6796	1846	95796	
1988-1989	1094	517	1209	4366	11593	14787	14905	14916	13099	11788	6926	2876	98076	
Column Total	1876	875	2050	9316	22534	29304	29702	29764	26649	23358	13722	4722		
													Grand Total	193872

### Expected Values

Frozen Land July	Aug	Sep	Oct	Nov	Dec	Jan	Feb	Mar	Apr	May	June	
1997-1998	926.9688	432.355	1012.95	4603.22	11134.5	14480	14676	14707	13167.799	11541.7	6780.31	2333.2
1988-1989	949.0312	442.645	1037.05	4712.78	11399.5	14824	15026	15057	13481.201	11816.3	6941.69	2388.8
1997-1998	22.6717	12.7873	29.1875	26.12435	3.362596	0.0961	0.9919	1.3521	11.093524	0.06963	0.0363	101.75
1988-1989	22.14464	12.49	28.5089	25.51703	3.284425	0.0939	0.9688	1.3207	10.83563	0.06801	0.03545	99.381

414.1669 with df 11

### Observed Values

Non-Frozen   July	Aug	Sep	Oct	Nov	Dec	Jan	Feb	Mar	Apr	May	June	Row Total		
1997-1998	16473	17417	16802	12614	6523	3394	2191	2424	2807	6257	11102	15852	113856	
1988-1989	16151	17247	16425	13189	5861	3081	2064	2309	3309	5953	10961	14809	111359	
Column Total	32624	34664	33227	25803	12384	6475	4255	4733	6116	12210	22063	30661		
													Grand Total	225215

### Expected Values

Non-Frozen   July	Aug	Sep	Oct	Nov	Dec	Jan	Feb	Mar	Apr	May	June	
1997-1998	16492.85	17524.2	16797.7	13044.54	6260.652	3273.4	2151.1	2392.7	3091.9046	6172.69	11153.8	15500
1988-1989	16131.15	17139.8	16429.3	12758.46	6123.348	3201.6	2103.9	2340.3	3024.0954	6037.31	10909.2	15161
1997-1998	0.0239	0.65532	0.0011	14.21022	10.99351	4.4436	0.7405	0.4085	26.252632	1.15163	0.24064	7.9721
1988-1989	0.024436	0.67001	0.00113	14.52886	11.24002	4.5432	0.7571	0.4176	26.841294	1.17745	0.24604	8.1509

135.6918 with df 11

Note: NFBG = Non-Frozen Bare Ground  
 FBG = Frozen Bare Ground  
 NFBG = Non-Frozen Snow Cover  
 FSC = Frozen Snow Cover